THE SYSTEMATICS OF SULFIDE MINERALOGY

IN THE

REGIONALLY METAMORPHOSED AMMONOOSUC VOLCANICS

by

SIMON MUIR PEACOCK

B.S., Massachusetts Institute of Technology
(1981)

SUBMITTED TO THE DEPARTMENT OF
EARTH AND PLANETARY SCIENCES
IN PARTIAL FULFILLMENT OF
THE REQUIREMENTS FOR
THE DEGREE OF

MASTER OF SCIENCE IN
EARTH AND PLANETARY SCIENCES

at the

MASSACHUSETTS INSTITUTE OF TECHNOLOGY

JUNE 1981

Signature of Author _____
Department of Earth and Planetary Sciences
May 22, 1981

Certified by _____
Frank S. Spear
Thesis Supervisor

Accepted by _____
Theodore R. Madden
Chairman, Departmental Graduate Committee

THE SYSTEMATICS OF SULFIDE MINERALOGY

IN THE

REGIONALLY METAMORPHOSED AMMONOOSUC VOLCANICS

by

SIMON MUIR PEACOCK

Submitted to the Department of Earth and Planetary Sciences
on May 26, 1981 in partial fulfillment of the
requirements for the Degree of Master of Science in
Earth and Planetary Sciences

ABSTRACT

Sulfide-bearing amphibolites, from the Ammonoosuc Volcanics, E. Vermont and W. New Hampshire, representing a range in metamorphic grade from middle greenschist to upper amphibolite facies, were investigated to determine the behavior of sulfides during regional metamorphism.

Modal analyses of 150 samples document the conversion of pyrite to pyrrhotite with increasing metamorphic grade. A detailed petrographic study of twenty-seven pyrrhotite-bearing samples revealed three distinct iron-sulfide textures, believed to represent prograde (pyrite --→ pyrrhotite), retrograde (pyrrhotite --→ marcasite), and polymetamorphic (marcasite --→ secondary "pyrite") reactions. Microprobe analyses of pyrite-pyrrhotite pairs indicate the iron-sulfide geothermometer may be of some use in determining relative metamorphic grades, but absolute temperatures cannot be accurately determined.

The occurrence of pyrite in equilibrium with pyrrhotite over a wide range in metamorphic grades strongly suggests that temperature is not the dominant controlling factor in the pyrite --→ pyrrhotite reaction. The positive correlation observed between marcasite alteration of pyrrhotite and pyrite-bearing samples, along with other textural and mineral-chemical data, support a desulfurization mechanism. The conversion of pyrite to pyrrhotite is driven by the flow of sulfur-poor fluids through the rock, in a similar manner to the desulfurization mechanism recently proposed for metapelites from Maine (Ferry, 1981).

The documentation of sulfur transport during metamorphism has important implications for sulfide ore exploration. If the path of the sulfur could be traced, then new ore deposits may be discovered where the sulfur was deposited.

TABLE OF CONTENTS

LIST OF FIGURES

LIST OF TABLES

ACKNOWLEDGEMENTS

"Well, the first days are the hardest days,
Don't you worry any more?
Cause when life looks like easy street
There is danger at your door."

J. Garcia (pers. comm.)

There are many people who have contributed, directly and indirectly, to the successful (?) completion of this thesis. With the final "final" deadline only hours away, it would be impossible to thank everyone. I apologize to those that time and space do not allow me to mention individually, but I appreciate everything they have done for me.

First, I'd like to thank Frank Spear for being my advisor in this research project and for turning me on to metamorphic petrology. His colorful and creative discussions on n-composition space have greatly increased my understanding of rocks. His signature on the title page is also greatly appreciated.

My parents deserve special thanks, after all, it was their idea in the first place. I apologize to both of them for not choosing a more understandable career. My parents and grandparents lent me moral support over the past four years, for which I am eternally grateful. Some may live an ocean away, but they were always beside me.

I am deeply indebted to those who came to my rescue in the closing minutes of the final hour. Their names belong on the title page as much as my own, but its already typed. Dave Gerlach taught me the art of photography and gave me much

encouragement over the past two weeks. Tim Peacock typed the bulk of the seemingly endless appendices and tables. He may be my brother, but he's still a pretty decent guy. Ed Wooten typed the fascinating references and commented on several Grateful Dead tapes.

I'd like to express my thanks to all my friends, without whom none of this would have been possible. Especially - to Andy and Dave, for putting up with my rock gardens on the coffee table for four years - to Al, who helped me deal with the concept of reality - to Peter and Penny, for their inspiring joint discussions about life and the electron microprobe - to Chrystal, for keeping me going eight days a week - to Jerry, Bob, Phil, Brett, Bill, and Mickey, for years of fascination and inspiration - and finally, to Lew Gosmon, Bucko, and all the Dekes, for the best four years of my life.

Electron microprobe funds were provided by the Mining and Minerals Resource Research Institute (as an undergraduate) and the geology department's Student Research Fund (as a graduate student). Sample preparation and other miscellaneous costs were covered by Dr. F.S. Spear's NSF Grant #EAR-79-11166.

"Sometimes the lights all shine in on me,
Other times I can barely see,
Lately it occurs to me,
What a long strange trip its been."

J. Garcia (pers. comm.)

I. INTRODUCTION

Sulfides are common, though usually minor, constituents of many volcanic and sedimentary rocks and their metamorphosed equivalents. Phase relations in the binary Fe-S system have been studied experimentally. In particular, extensive investigations of pyrite-pyrrhotite equilibria have been done by Toulmin and Barton (1964) and Arnold (1962). Extensive literature exists on sulfide ore deposits because of their economic value. The effects of metamorphism on sulfide ore deposits have been capably reviewed by McDonald (1967) and Vokes (1968).

The effects of metamorphism on disseminated sulfides in sedimentary rocks have been investigated by several workers. A pyrite --→ pyrrhotite "isograd" has been mapped in pelitic schists from Maine by Williamson and Myer (1969), and from Tennessee and North Carolina by Carpenter (1974). Systematic relationships between Fe-Mg mineral compositions and coexisting sulfides have been observed in metapelites from Massachusetts (Robinson and Tracy, 1976) and Maine (Guidotti et al., 1976). Most recently, Ferry (1981) has proposed a desulfurization reaction mechanism that is thought to be responsible for the conversion of pyrite to pyrrhotite in graphitic metapelites from south-central Maine.

The question of sulfur mobility during metamorphism has been debated in the literature. One side claims that no significant transport of sulfur occurs during metamorphism

(e.g. Thompson, 1972; Robinson et al., 1976), while the other side contends that sulfur is often mobilized in a metamorphic event (e.g. Fullagar et al., 1967; Ferry, 1981).

Disseminated iron sulfides are common in the regionally metamorphosed Ammonoosuc Volcanics and almost all sulfur in the volcanics is contained by the iron sulfides. Therefore, by studying the behavior of iron sulfides in the Ammonoosuc Volcanics, insight should be gained into the behavior of sulfur during metamorphism.

Studies of disseminated sulfide behavior in regionally metamorphosed volcanic rocks are rare. To my knowledge, only two such studies have been reported in the literature by Banno and Kanehira (1961) and Kanehira et al. (1964). They observed a pyrite to pyrrhotite transition with increasing metamorphic grade in basic schists from several Japanese metamorphic terrains. In several other metamorphic terrains, they were unable to document such a transition.

In the past ten years, as some of the larger sulfide deposits in the western United States have been exhausted, mining companies have returned to the Appalachian Mountains to look over old prospects with new geophysical techniques. Recently, massive sulfide deposits have been discovered on the sea floor in volcanic rocks, thereby strongly suggesting that volcanic activity and massive sulfide deposition are interrelated. The Ammonoosuc Volcanics are one of several volcanic units in the Appalachians that were formed on the sea floor and have been metamorphosed during their emplacement

onto the North American continent. If sulfur is mobilized during metamorphism, then disseminated sulfides and sub-economic sulfide deposits could possibly be concentrated into valuable ore deposits. Thus, the behavior of sulfur and sulfides in metamorphosed volcanic rocks has important economic consequences.

Goals

The primary objective of my research and this report is to understand the behavior of the sulfide phases observed in the regionally metamorphosed Ammonoosuc Volcanics. The specific aims of my research were:

1) To describe and interpret the sulfide textures observed in the Ammonoosuc Volcanics.

2) To analyze the various sulfide phases with the electron microprobe and determine if any systematic changes in mineralogy occur with increasing metamorphic grade.

3) To document the pyrite --→ pyrrhotite transition in metavolcanics, if indeed one could be documented.

4) To evaluate the usefulness of the pyrite-pyrrhotite geothermometer using microprobe analyses of pyrite-pyrrhotite assemblages.

In addition, sulfide mineral-chemical and textural observations were combined with pyrite-pyrrhotite geothermometry in attempts place constriants on the:

5) metamorphic thermal history of a poorly understood suite of rocks.

6) extent of sulfur mobility in the Ammonoosuc Volcanics.

7) mineral reaction responsible for the pyrite-pyrrhotite transition.

Geologic Setting

The Ammonoosuc Volcanics are believed to be back-arc submarine volcanics deposited in the Middle Ordovician (~465 m.y.). The volcanics crop out in an area roughly 350 km long and 40 km wide in New England, with the long axis of the band roughly paralleling the Vermont/New Hampshire state line (see Figure 1). The Ammonoosuc Volcanics rest unconformably (?) on or intrude basement igneous gneisses of the Oliverian magma series, or in some areas overlie semipelites of the Albee Formation. Overlying the Ammonoosuc Volcanics is the Partridge Formation which consists of graphitic and pyrrhotitic mica schists. The Partridge Formation is interpreted to be metamorphosed marine shales deposited in a strongly reducing environment (Thompson et al.,1968). A complete stratigraphic section for western New Hampshire is shown in Figure 2, but not all formations are continuous throughout the study area.

The Middle Ordovician age for the Ammonoosuc Volcanics was deduced from three, rather tenuous, lines of reasoning:

1) Ordovician graptolites are observed in black slates in the Cupsuptic Quadrangle (west central Maine) that are thought to correlate with the Partridge Formation (Harwood,

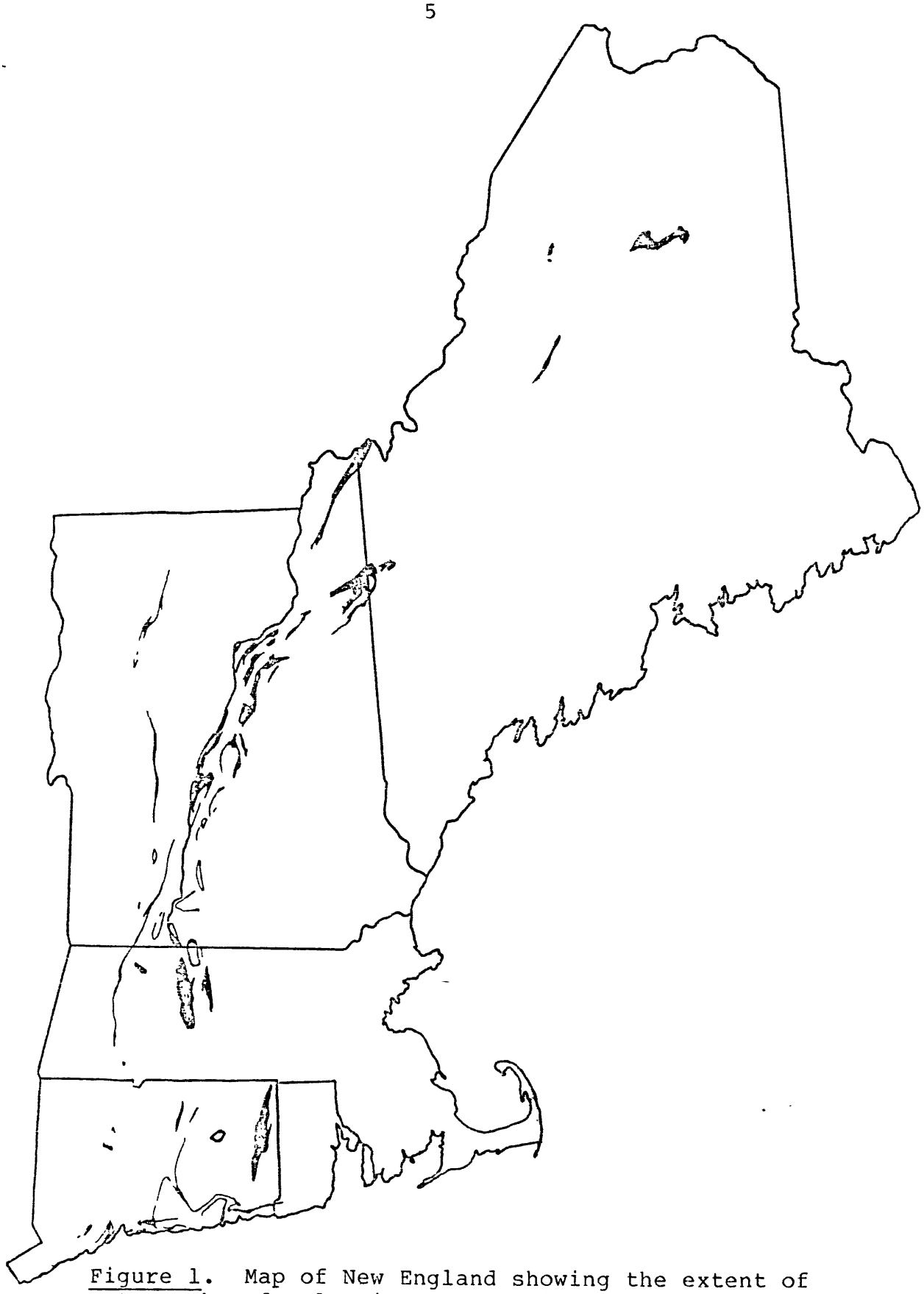

Figure 1. Map of New England showing the extent of metamorphosed volcanic rocks similar to the Ammonoosuc Volcanics.

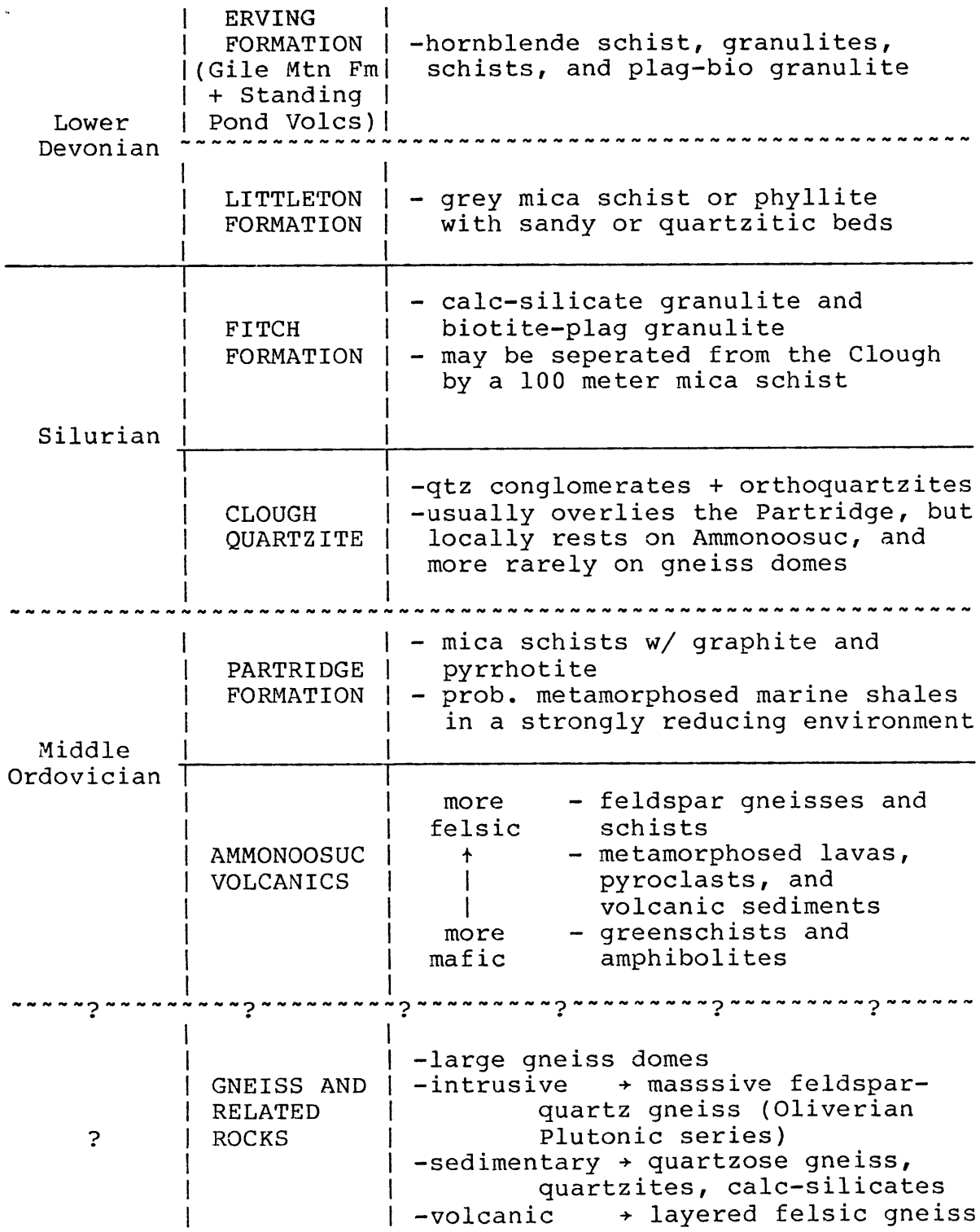

Figure 2. Paleozoic stratigraphy and lithologies of western New Hampshire.

1966; Harwood and Berry, 1967; Green and Guidotti, 1968).

2) Further to the northeast near Somerset Junction, Maine, Ammonoosuc-like rocks contain shelly fossils that indicate an earlier Middle Ordovician age (Boucot, 1961).

3) The Partridge Formation and the Ammonoosuc Volcanics are believed to correlate in eastern Vermont with the Cram Hill Formation and Barnard Volcanics, respectively (Billings, 1956; Doll et al., 1961). The Cram Hill and Barnard units can be traced into Canada where middle Ordovician graptolites are observed in the Cram Hill Formation in Beauceville, Quebec (Cady, 1960; Berry, 1962).

The Ammonoosuc Volcanics consist of metamorphosed lavas, pyroclastics, and volcanic sediments. Relict primary features such as pillow lavas, agglomerates, volcanic breccias, and amygdules can be recognized. The volcanics range in composition from rhyolites to basalts. Mafic volcanics are more common towards the base of the sequence, while felsic volcanics are dominant in the upper half. The Ammonoosuc crops out in a variety of habits ranging from massive to finely-bedded.

The Ammonoosuc Volcanics were regionally metamorphosed in the Acadian Orogeny (Devonian) and possibly the Taconic Orogeny (Ordovician). The mafic volcanics have been metamorphosed to greenschists and amphibolites, while the more felsic volcanics are now biotite-feldspar gneisses and schists. Anthophyllite and cummingtonite amphibolites are common throughout the area, particularly in the lower part of

the section. Manganiferous, garnetiferous rocks (coticules), possibly representing metamorphosed chert, are locally observed, as are calc-silicates.

Methods of Investigation

Approximately 250 amphibolites collected from the Ammonoosuc Volcanics by F.S. Spear were checked for the presence of sulfides. Seven suites of rocks containing sulfide-rich amphibolites were chosen, representing a range in metamorphic grade from the middle greenschist to upper amphibolite facies. From these suites, twenty-seven polished thin-sections containing pyrrhotite were chosen for detailed study. Reflected and transmitted light microscopy was used to identify mineral assemblages and interpret textures. M.I.T.'s automated electron microprobe was used to determine the chemical composition of sulfides and other selected phases. Modal amounts of sulfides were estimated for 150 samples chosen at random from the seven suites. In addition, polished slabs were made from greenschist facies Ammonoosuc Volcanics collected by the author and sulfide modes were estimated in order to further document the pyrite --→ pyrrhotite transition in the Ammonoosucs.

The term "spot" is used throughout this report to define a circular area, 2 mm in diameter, on a polished thin-section that contains one or more sulfide grains. It was arbitrarily assumed, unless proven otherwise, that phases in the same "spot" were in equilibrium. Sulfide grains that are

in the same "spot", but not in actual contact with each other, are distinguished by a simple labelling system. As an example, A, B, and C are distinct sulfide-bearing "spots" on a polished thin-section; A, AA, and AAA are three non-touching sulfide grains in "spot" A.

Sample Localities and Peak Metamorphic Temperatures

The seven suites analyzed with the electron microprobe were collected by Dr. F.S. Spear during the summers of 1973, 1977, and 1980 as part of his ongoing study of the Post Pond and Ammonoosuc Volcanics. A eighth suite (Interstate 91) was collected by the author during the summer of 1980. Polished slabs were made for modal analyses, but no chemical analyses were carried out on this suite. The location of the eight suites are shown in Figure 3. Table 1 lists the sample numbers that make up the eight suites, and the approximate peak metamorphic temperatures determined from the silicate and oxide assemblages. The temperature estimates for each suite are probably accurate to $\pm$20°C. Each suite and the evidence used to estimate the peak temperatures will be discussed in order of increasing metamorphic grade.

Interstate 91. Seventeen samples (80-J1→11, 80-K1→6) were collected from road cuts alongside two Interstate 91 exit ramps (Hanover 7.5' Quadrangle). The 80-J suite was collected at the Hanover exit, and the 80-K suite was collected from the White River Junction turnoff (exit 11). Both suites lie on the west side of the Ammonoosuc Fault, in the Post Pond

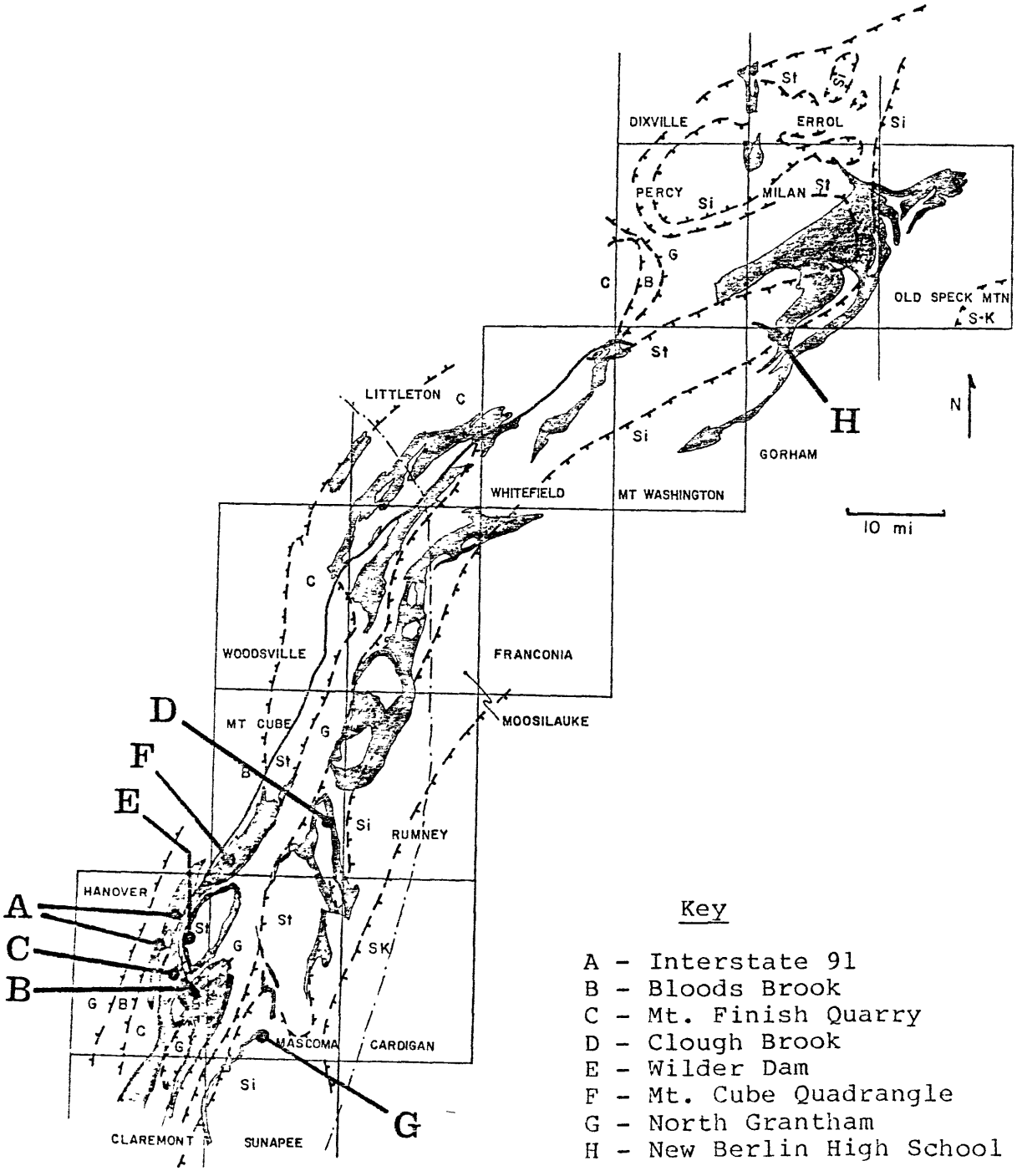

Figure 3. Sample locations in western New Hampshire and eastern Vermont.

Suite Name	Sample #'s	Estimated Peak Temperature of Metamorphism
Interstate 91	80-J's 80-K's	450°C
Bloods Brook	77-21→32	465°C
Mt. Finish Quarry	77-15's	480°C
Clough Brook	77-18's	510°C
Wilder Dam	77-20's	510°C
Mt. Cube Quadrangle	73's 77-58D	535°C
North Grantham	80-28's	575°C
New Berlin High School	80-70's	? (polymetamorphic?)

Table 1. The eight suites, sample numbers, and estimated peak temperatures achieved during regional metamorphism (± 20°C).

Volcanics (the stratigraphic equivalent of the Ammonoosuc Volcanics in western New Hampshire and eastern Vermont (Thompson et al., 1968).

The Interstate 91 suite lies only 3 km southwest of the 77-23 locality (Bloods Brook). The Ammonoosuc Fault runs between the two suites, seperating lower grade rocks on the west from higher grade rocks on the east. Therefore the peak metamorphic temperature of the Interstate 91 suite should be lower than Bloods Brook. The I-91 suite lies below the garnet isograd and contains actinolite + epidote + chlorite + albite suggesting lower-middle greenschist metamorphism. The peak temperature of metamorphism was therefore estimated to be ~450°±20°C.

Bloods Brook. One sample (77-23D) was analyzed from the Bloods Brook suite collected by Dr. F.S. Spear. The suite was collected from outcrops in Bloods Brook, south of the Grafton County line (North Hartland 7.5' Quadrangle).

The Bloods Brook suite lies below the garnet isograd, but this may be a function of the rocks' bulk composition. The metamorphic grade is at least as high as the greenschist-amphibolite facies boundary, since hornblende is present, but below the albite-oligoclase isograd. The best estimate that can be made is that the Bloods Brook suite is probably 10-20°C cooler than the Mt. Finish Quarry. Thus, a metamorphic peak temperature of 465±20°C is estimated for the Bloods Brook suite.

Mt. Finish Quarry. A suite of samples was collected from the Mt. Finish Quarry located ~400 meters WNW of the Mt. Finish summit (North Hartland 7.5 Quadrangle). The Ammonoosuc crops out as well-bedded massive amphibolites and leucocratic rocks, with interbedded cherts. Disseminated sulfides occur thoughout the rocks and fill fractures that parallel the bedding surfaces. Only one sample (77-15Y) contained pyrrhotite, thus it was the only one analyzed with the electron microprobe.

The quarry lies only 2 km WNW of the 77-23 outcrop, but apparently reached a slightly higher grade as evidenced by the presence of garnet. Oxygen-isotope studies done on quartz-magnetite pairs by D. Rumble at the Geophysical Laboratory indicate a peak metamorphic temperature of 480±20°C (using the calibration of Downes and Deines, 1978) which is consistent with the observed mineral assemblage.

Clough Brook. The Clough Brook suite was collected from a 2.5 km traverse along the Clough Branch, a brook that runs down the southeast side of Smarts Mountain (Smarts Mtn. 7.5' Quadrangle). Most of the rocks are garnet amphibolites. Four samples (77-18M, O, P, and X1) were analyzed from the suite.

Garnet-biotite (Ferry and Spear calibration, 1978) suggest a 510±20°C peak metamorphic temperature, consistent with the observed mineral assemblage.

Wilder Dam. A suite of rocks (77-20's) was collected by Dr. F.S. Spear from a quarry located 0.5 km south of the Wilder

Dam, 100 meters east of Route 10 (Hanover 7.5' Quadrangle). The 77-20 quarry lies approximately 7.5 km due north of the Bloods Brook locality.

Samples in the Wilder Dam suite contain staurolite, indicating a higher metamorphic grade than the Mt. Finish Quarry, probably close to the temperature of the Clough Brook suite. Consequently, the peak metamorphic temperature is estimated at ~510°±20°C (the same as Clough Brook).

Mt. Cube Quadrangle. Eight samples were analyzed from three seperate localities in the southwest corner of the Mt. Cube Quadrangle. Five samples (73-22E, 25A, 25B, 26A, and 27C) are part of a larger suite collected from a ~250 meter long road cut along U.S. Route 5. Two samples (73-30M and 73-31B) were collected from two quarries seperated by 0.5 km, located west of I-91 and north of the Ompompanoosuc River. The eighth sample (77-58D) was collected on Wilmot Mountain.

Garnet-biotite and quartz-magnetite geothermometry indicate a peak temperature of metamorphism of 535°±20°C for the localities in the Mt. Cube Quadrangle suite.

North Grantham. Five samples were analyzed from a suite of rocks collected near North Grantham, between exits 13 and 14 of Interstate 89, just west of Route 10 (Mascoma 15' Quadrangle). The stratigraphic thickness of the volcanics in the outcrop is thinner than observed elsewhere - presumably due to either depositional controls or tectonic thinning. Both the mafic (lower) and felsic (upper) units are exposed.

Sillimanite is observed in nearby metapelites,

indicating that the North Grantham suite lies within the sillimanite zone. The garnet-biotite geothermometry data is widely scattered, but one sample (80-28W) shows relatively consistent values of 570-585°C. Thus, a peak temperature of 575°±20°C was assumed for the suite.

New Berlin High School. Six samples (80-70C, J, K, N, PP, and T) were analyzed from a rock cut exposed on the north and east sides of the new Berlin High School (Berlin 7.5' Quadrangle). The outcrop is approximately 75 meters across and the bedding dips steeply (75°) to the east.

The metamorphic thermal history of this suite is unknown, and one of the goals of this research is to see if any clues could be uncovered about its history from the observed sulfide assemblages, textures, and chemical compositions. Polymetamorphic rocks are observed not far to the northeast, suggesting that the new Berlin High School may have also undergone polymetamorphism.

II. MINERALOGY

Twenty-seven polished thin-sections were examined with the aid of the petrographic microscope under transmitted and reflected light. Table 2 tabulates the silicate and oxide assemblages in order of decreasing modal abundance for each sample. Sulfide assemblages, estimated modal abundances, pyrrhotite compositions, and the degree of marcasite alteration for each sample is tabulated in Table 3.

Sulfides

Pyrrhotite. Pyrrhotite is observed in all twenty-seven polished thin-sections, not surprising since only samples found to contain pyrrhotite in a preliminary search were chose for further study. Pyrrhotite has a creamy tan color (light yellow with a brownish-pink tinge) in reflected light. Under crossed nicols, pyrrhotite exhibits a strong, grey to deep red-brown, anisotropy. The polished surface is always pitted with small, anhedral voids, similar to those commonly observed in magnetite. Individual grains tend to be anhedral, rounded, and often elongate. Occasional subhedral grains are observed, but most straight pyrrhotite edges are defined by biotite grains and are not true crystal forms. Pyrrhotite grains often occur in disseminated bands that parallel the foliation in the rock. Individual grains are usually oriented with their long dimensions crudely parallel to the foliation. Anhedral aggragates of up to 5-10 grains are not uncommon.

SAMPLE	SILICATES Plg	Hbl	Bio	Chl	Qtz	Cum	Gar	OXIDES Ilm	Mag	MINOR PHASES
Bloods Brook										
77-23D	1	2	5	3				6	4	
Mt. Finish										
77-15Y	1	5	6	7	4	3	2		8	
Clough Brook										
77-18M	1		3			2				
77-18O	1	6	4	5		2	3	8	7	
77-18P	1	4	6			2	3		5	
77-18X1		1		2						ep,cc
Wilder Dam										
77-20G	1	2	3					4		cc,anth
77-20N	1	2		4		3		5		
Mt Cube Quad										
73-22E	1	2			3		4	5		sill
73-25A	2	3		5	1		4	6		cc
73-25B	2	1	5	6		4	3	7		st
73-26A	2	1		3						st,cc,ap
73-27C	4	1	2	5			3	6		
73-30M			2		1					mu
73-31B	2	1	3		4			5		ap,ep,sph
77-58D	1	3			2					anth,ged
N. Grantham										
80-28O	2	1	3		4			5		
80-28T	1		2	4			3	5		
80-28U	2	1								
80-28W	1		3	4		2	5	6		anth,ged
80-28X	1	4		2		5	3			
New Berlin HS										
80-70C	1		2				3			
80-70J	1		2	3					4	anth,ged
80-70K	1		2	3						anth,ged
80-70N	1		2	3						anth,ged
80-70PP	2		4	5	1		6		3	cord,st
80-70T	1	2	3	4						

Abbrev. - anthophyllite(anth), apatite(ap), biotite(bio), calcite(cc), chlorite(chl), cordierite(cord), cummingtonite (cum), epidote(ep), garnet(gar), gedrite(ged), hornblende(hbl) ilmenite(ilm), magnetite(mag), muscovite(mu), plagioclase(plg) quartz(qtz), sillimanite(sill),sphene(sph),staurolite(st).

Table 2. Silicate and oxide assemblages of the twenty-seven polished thin-sections. Numbers refer to relative modal abundances (1 - most common, ... etc.)

SAMPLE	MODAL ABUNDANCES PY	PO	CPY	OTHER SULFIDES	Po N_{FeS}	MARCASITE ALTERATION
Bloods Brook						
77-23D	++	++	+		0.945	slight
Mt. Finish						
77-15Y	+	++	+		0.936	none
Clough Brook						
77-18M	+	+	+		0.944	sl to mod
77-18O	o	+	+		0.933	none
77-18P	o	+++	+		0.945	none
77-18X1	++	+	+	pent	0.924	none
Wilder Dam						
77-20G	o	++	+		0.945	none
77-20N	o	+	+		0.932	none
Mt Cube Quad						
73-22E	+	++	+		0.933	moderate
73-25A	++	++	+		0.932	none
73-25B	++	+	+		0.938	none
73-26A	o	+	+		0.933	moderate
73-27C	+	+	+		0.931	none
73-30M	o	++	+	aspy	0.945	slight
73-31B	+	++	+		0.935	none to sl
77-58D	++	++	+		0.930	sl to mod
N. Grantham						
80-28O	o	++	+		0.934	none
80-28T	o	++	+		0.929	none
80-28U	o	+++	+		0.932	none
80-28W	+	++	+		0.933	sl to mod
80-28X	+	+	+		0.943	sl to mod
New Berlin HS						
80-70C	++	+++	+		0.941	v. sl
80-70J	+++	++	+		0.939	v. sl
80-70K	+++	+++	+++		0.945	sl to mod
80-70N	++	++	+		0.937	sl
80-70PP	++	+++	++		0.955	none to sl
80-70T	++	+++	++		0.939	none to sl

Abbrev. - arsenopyrite (aspy), chalcopyrite (cpy), pentlandite (pent), pyrite (py), pyrrhotite (po).

o - not present ++ - common mod - moderate

\+ - rare (<2%) +++ - abundant sl - slight

v. sl - very slight

Table 3. Sulfide assemblages, approximate modal abundances, pyrrhotite compositions, and degree of marcasite alteration for the 27 polished thin-sections.

The pyrrhotite grain size is constant through all metamorphic grades, ranging from 0.025 to 1.0 mm within a single sample, and averaging 0.25 mm in diameter.

Pyrite. Pyrite is present in eighteen of the twenty-seven samples (two-thirds). It is a very bright, brassy yellow-white color in plane polarized (reflected) light and is isotropic or very slightly anisotropic under crossed polars. Pyrite shows a strong tendency to form euhedral crystals. This observation has been reported by many workers (e.g. Ramdohr, 1969) and has been attributed to its relatively high interfacial energy by Stanton (1964). The pyrite crystals are often cubes which yield square, rectangular, triangular, and hexagonal outlines. Rounded, subhedral pyrite grains are less common. Pyrite takes a high polish and, in contrast to pyrrhotite, is typically free of pits and voids. Small chalcopyrite inclusions are common; inclusions of other phases are rare. Secondary pyrite is observed in the New Berlin High School suite and will be discussed in detail in Chapter IV.

No systematic variation in grain size is observed with increasing metamorphic grade, in contrast to the increase in pyrite grain size frequently observed in metapelites (McDonald, 1967; Carpenter, 1974). Pyrite crystals vary from 0.05 to 1.0 mm in diameter in each sample, and average about 0.25 mm. Grains up to 3 mm in diameter are seen in 80-70J and 80-70K, possibly indicating a late stage or emplacement as a hydrothermal vein. The larger pyrite grains are often cracked indicating brittle deformation. In two samples, 77-15Y and

77-18X1, pyrite is partially altered (<5%) to a grey isotropic mineral, presumably limonite.

Marcasite. In fourteen samples, marcasite is observed replacing pyrrhotite to varying degrees. The replacement texture will be discussed in detail in the Chapter on "Sulfide Textures". Under plane light, marcasite is very similar to pyrite in color, but a slight greenish tinge is usually associated with marcasite. In crossed polars, marcasite displays extreme, deep blue to deep red, anisotropy. Marcasite is extremely fine-grained (<0.001 mm), and may be intermixed with very fine-grained pyrite and magnetite (Ramdohr, 1969). "Large" twinned marcasite crystals, up to 0.075 mm across are seen in one sample (80-28W).

Chalcopyrite. Chalcopyrite is present in all twenty-seven samples, presumably stabalized by the trace amounts of copper in the rocks. It appears deep brassy-yellow in plane polarized light and isotropic to weakly anisotropic under crossed polars. The smooth polished surface is frequently spoiled by abundant anhedral voids, very similar to the surface texture of pyrrhotite. Chalcopyrite is always anhedral and roughly equidimensional. It usually occurs as inclusions in pyrite in pyrrhotite, and rarely, by itself. Grain diameters average 0.1 to 0.2 mm in all suites, ranging from 0.02 to 0.4 mm. Exceptionally large grains, up to 2 mm across, are present in the New Berlin High School suite.

Pentlandite. A single anhedral pentlandite grain is present in 77-18X1. In plane light it is a light cream color, slightly paler and brighter than pyrrhotite, and lacking pyrrhotite's pinkish-brown tint. Under crossed polars, it is isotropic.

Arsenopyrite. Sample 73-30M contains several euhedral grains of arsenopyrite, 0.1 to 0.4 mm in diameter. It takes the same form as pyrite, but is whiter and exhibits strong red to blue anisotropy under crossed polars.

Silicates

Feldspars and Quartz. Twenty-five of the twenty-seven samples contain plagioclase feldspar - 77-18X1 and 73-30M are the only exceptions. Anhedral, equidimensional plagioclase grains frequently make up the matrix of the rocks. Grain diameters typically range from 0.01 to 0.5 mm, but 2 mm plagioclase grains are observed in the North Grantham suite. Polysynthetic twinning is common, as are zoned crystals with the cores typically altered to sericite.

Quartz is found in eight samples as anhedral, equant grains, 0.01 to 1 mm in diameter. The quartz grains typically occur in blebs or lenses parallel to the foliation. The larger quartz grains are often strained and appear to be recrystallizing to smaller, more mechanically stable, grains - a typical "mortar" texture.

No potassium feldspar was observed in any of the samples.

Amphiboles. Eighteen samples contain hornblende, usually as anhedral, elongate prisms. Hornblende makes up more than 95% of sample 77-18X1. Hornblende prisms are generally 0.05 to 1 mm long, though sprays up to 10 mm in length are common in the Mt. Cube Quadrangle suite. Blue-green pleochroism is displayed by most of the hornblendes, except for olive-green pleochroism seen in the New Berlin High School suite. Many hornblende grains are poikiloblastic, with plagioclase inclusions being common. The long axes of the hornblende grains usually define a lineation.

Cummingtonite is observed in eleven samples. It occurs as anhedral prisms up to 5 mm long, exhibiting very pale green pleochroism. In about half of the cummingtonite-bearing samples, the cummingtonite prisms are extremely thin, almost needle-like, which lie within the biotite foliation. Poikiloblastic textures are observed in several samples - a spectacular example of this texture is seen in 77-20N.

Orthoamphiboles (anthophyllite and gedrite) occur in three samples in sprays up to 5 mm long. The grains show frequent basal partings and pale yellow to pale green pleochroism.

Sheet Silicates. Biotite is a common phase in the Ammonoosuc Volcanics, occurring in nineteen samples. It forms anhedral to subhedral tabs that define a foliation in the rocks (parallel to the hornblende fabric). The grains typically range from 0.01 to 1 mm in length, with 2 mm long tabs common in the North Grantham suite. Red-orange pleochroism is

observed in all suites, except for biotite in the Mt. Cube Quadrangle which is brownish-green. Pleochroic halos caused by zircon inclusions are common.

Subhedral muscovite tabs up to 0.3 mm long are seen in 73-30M. This is the only muscovite-bearing sample in the twenty-seven samples studied.

Chlorite grains are present in sixteen samples, and in some cases both prograde and retrograde textures are observed. Chlorite occurs as subhedral or anhedral tabs (0.05 to 0.5 mm long) that frequently cut across the biotite-hornblende fabric. In some samples, chlorite is seen replacing biotite and/or hornblende grains, in which case it is interpretated as being a retrograde mineral.

Garnet. Pale pink garnets (almandine) are observed in eleven samples. They are subhedral to euhedral with six-sided cross-sections. Grains up to 1 cm across are seen. The garnets are almost always poikiloblastic with plagioclase and quartz inclusions common. Extremely poikiloblastic garnets with rotated inclusion trails are observed in 77-15Y. Garnets with poikiloblastic cores and inclusion-free rims indicating two different growth rates are not uncommon.

Staurolite. Stubby staurolite prisms are found in three samples. The anhedral to euhedral grains range up to 0.75 mm in length. Their long directions show no clear relation to the foliation. In two samples staurolite occurs as inclusions in garnet.

Minor phases. Epidote, apatite, and cordierite are also observed in several samples. Cordierite makes up approximately five percent of 80-70PP. The other silicate phases occur in relatively minor or trace amounts in the samples (see Table 2).

Oxides

Two oxide phases are commonly observed in the Ammonoosuc Volcanics - magnetite and ilmenite. Magnetite is common in the three lowest-grade and polymetamorphic (?) suites, while it is virtually absent in the two high-grade suites. Ilmenite is commonly observed in samples from all six metamorphic grades. Limonite (goethite) is observed as a surficial weathering product of pyrite in two samples. Sphene is present in trace amounts in several samples.

Magnetite. Magnetite is observed in eight of the twenty-seven samples. The two highest-grade suites are virtually devoid of magnetite - only 80-28X contains magnetite. (Sample 80-28X shows abundant evidence for substantial retrograde metamorphism - almost all the hornblende has been retrograded to chlorite, while much of the pyrrhotite has been converted to marcasite.) Magnetite occurs as greyish-brown, isotropic or weakly anisotropic, equant grains. The grains show a strong tendency to form euhedral crystals, though rounded, subhedral grains are sometimes observed. Rounded, bleb-like pits typically mar the magnetite surface. In 77-23D, magnetite grains range from 0.01 to 0.15 mm in diameter. In all other samples, the magnetite grains average 0.5 mm across,

and range from 0.05 to 3 mm.

Ilmenite. Ilmenite is observed in twenty-five of the twenty-seven samples - only 77-15Y and 80-28V lack ilmenite. It is grey in color, lighter and less brown than magnetite, and exhibits very strong, light grey to deep red-brown, anisotropy. Ilmenite commonly forms small, subhedral elongate prisms with a length to width ratio of ~4:1. The long axis is generally aligned parallel to the biotite-hornblende foliation. In all suites ilmenite long axes average 0.1 to 0.2 mm, and range from 0.05 to 0.5 mm. No systematic variation in grain size is observed. In contrast to magnetite, ilmenite grains have a clean, unpitted surface when polished.

Carbonates

Calcite occurs as anhedral crystals in four samples. The grains range from 0.05 to 1 mm in diameter. Grains twinned along three different planes are common.

III. SULFIDE TEXTURES

Textures in metamorphic rocks are often the key to identifying reactions between silicate phases. Sulfide textures have been discussed in the literature more extensively than silicate textures, yet sulfide textures are the lesser understood of the two. In contrast to silicates, the softer sulfides like pyrrhotite and chalcopyrite have been shown to flow ductilly in response to metamorphic stresses (McDonald, 1967). To make matters worse, Stanton (1964) has shown that boundaries between sulfide grains are largely determined by their relative interfacial energies, or surface tensions. This implies that observed textures may have developed by recrystallization after the metamorphic event. In light of these considerations, a frozen reaction texture such as pyrrhotite pseudomorphically replacing pyrite is unlikely to be preserved.

Despite these difficulties, three distinct iron sulfide reaction textures can be identified in the Ammonoosuc Volcanics. The first involves euhedral pyrite reacting to form pyrrhotite and is interpreted to be a prograde reaction texture. The second consists of anhedral pyrrhotite being altered to fine-grained marcasite. This reaction is thought to occur during retrograde metamorphism. A third texture, observed in the New Berlin High School suite, is believed to represent the formation of secondary pyrite from marcasite, possibly as a result of polymetamorphism. The three textures

and their genetic implications will be discussed below.

"Prograde" Reaction Texture

Figures 4, 5, and 6 are prime examples of what is interpreted to be the prograde pyrite --→ pyrrhotite reaction texture. Seventeen of the twenty-seven samples have textures that are similar to those shown in the figures. In Figure 4, pyrite is being replaced by pyrrhotite along (100) crystallographic planes. This texture is thought to be the best example of a nearly-"quenched", or frozen, prograde reaction. Figures 5 and 6 are representative of the more commonly observed texture which is thought to represent a more slowly quenched pyrite --→ pyrrhotite prograde reaction. The slower cooling rate allows the small pyrite cubes time to anneal into a single euhedral grain. Some pyrite annealing even appears to have taken place in Figure 4 in the upper half of the photomicrograph. The strong tendency of pyrite to form euhedral crystals was discussed above and it therefore does not seem unreasonable for small pyrite grains to anneal into a single grain once the prograde reaction has stopped.

A common feature of the prograde texture is the partial or complete rimming of the pyrite grain by chalcopyrite as can be seen in both Figures 5 and 6. Initially, I thought that the chalcopyrite rim was evidence for pyrite being formed from pyrrhotite; any copper in the dissappearing pyrrhotite would form chalcopyrite because of the incompatibility of copper in the pyrite crystal lattice. Quick calculations show, however,

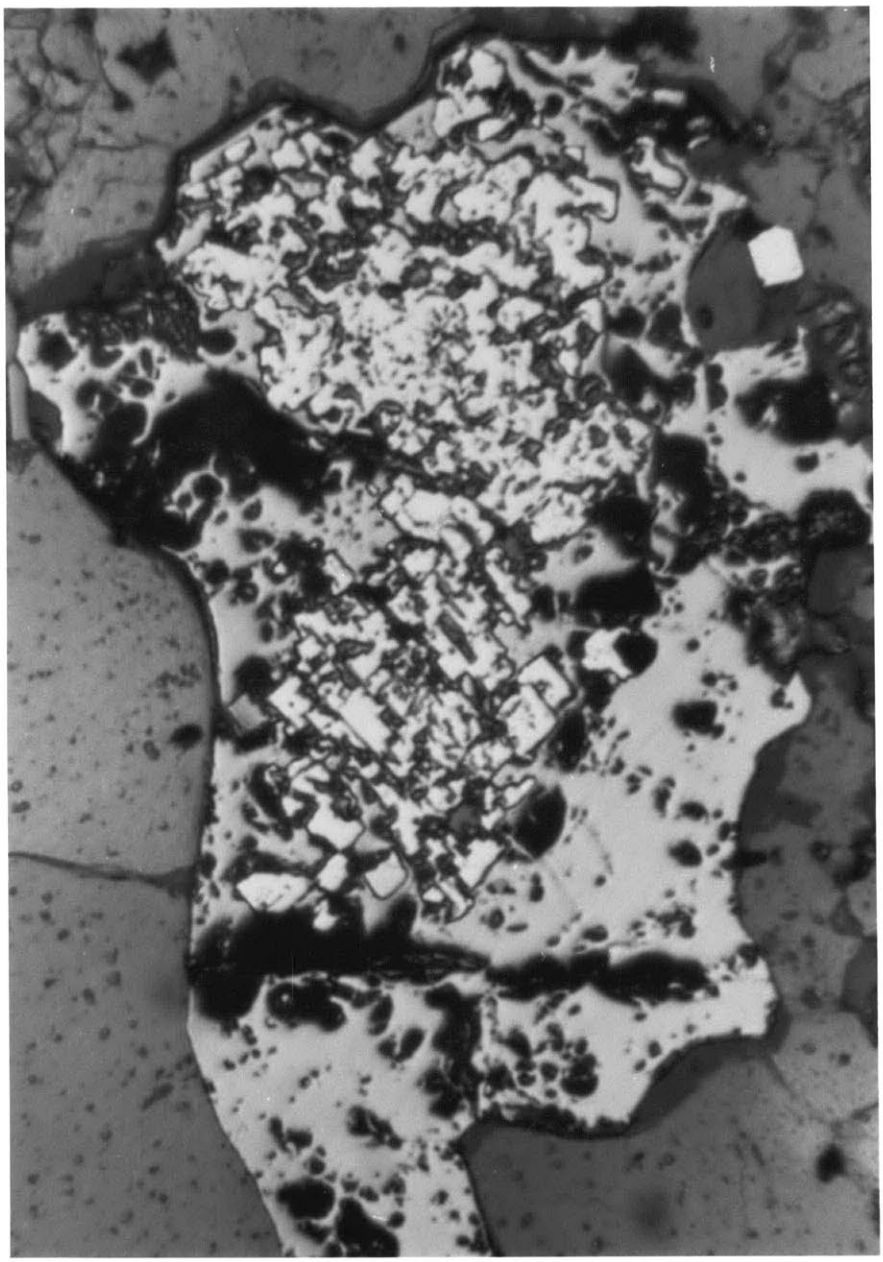

Figure 4. Quenched "prograde" reaction. Photomicrograph of sample 73-25A, "spot" A - field of view is 850 x 580 microns. Anhedral pyrrhotite (light grey) replacing pyrite (white) along (100) crystallographic planes.

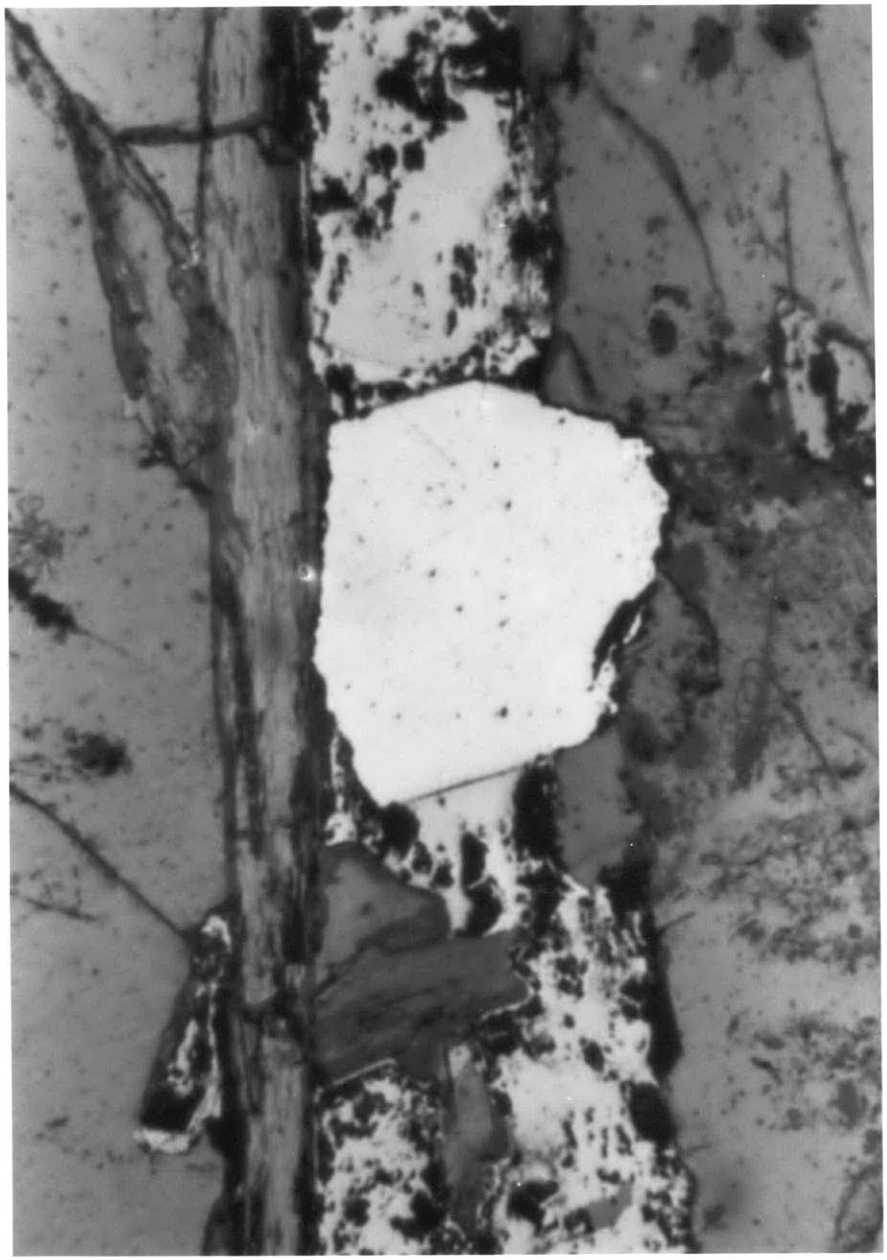

Figure 5. "Prograde" reaction. Photomicrograph of 77-18M, "spot" A - field of view is 780 x 560 microns. Large, euhedral pyrite grain (white), rimmed by chalcopyrite (very light grey), and set in elongate pyrrhotite grain (light grey). Note perfectly euhedral edges of pyrite against chalcopyrite.

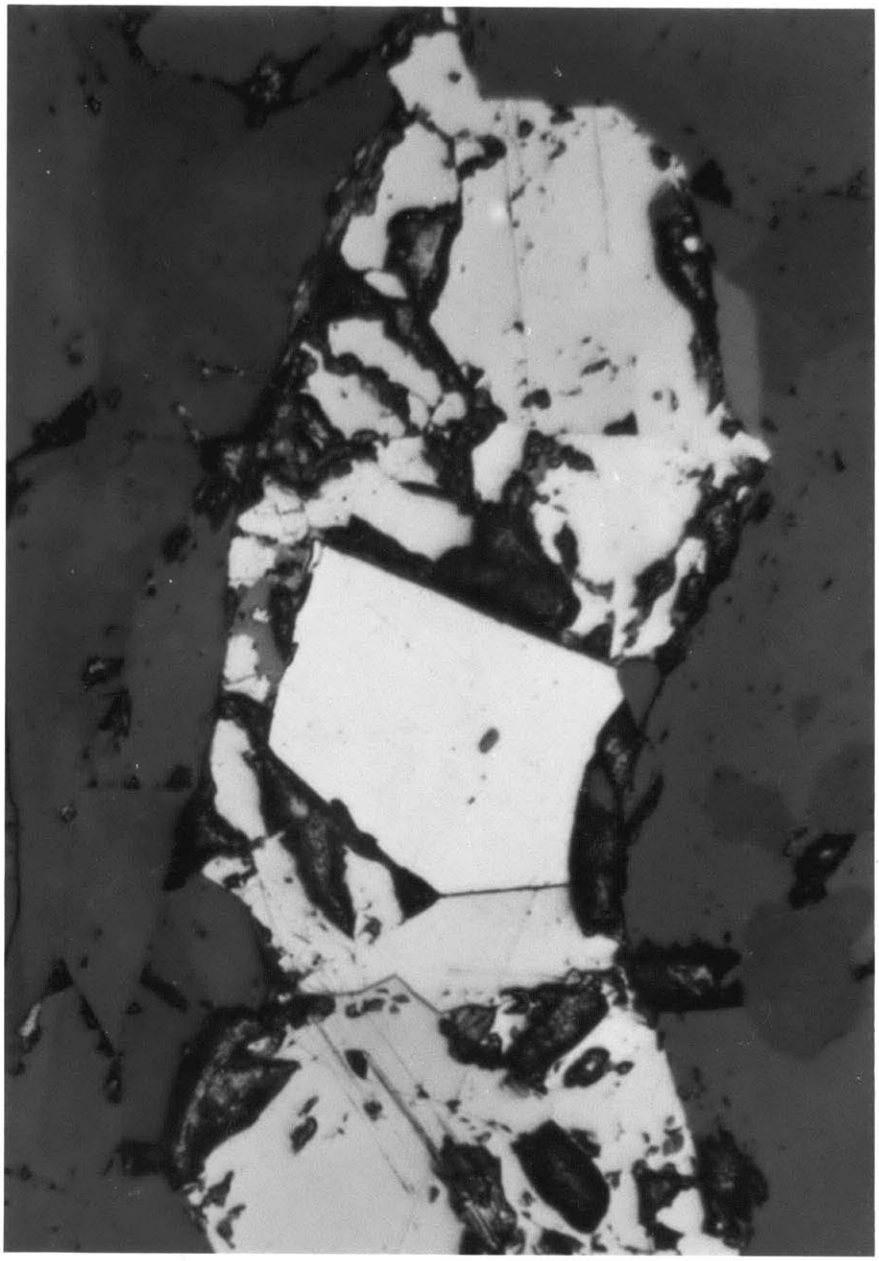

Figure 6. "Prograde" reaction. Photomicrograph of 73-31B, "spot" B - field of view is 310 x 220 microns. Euhedral pyrite (white), rimmed by chalcopyrite (slightly darker), set in elongate pyrrhotite grain (light grey).

that the amount of copper in the pyrrhotite is an order of magnitude less than is needed to account for the amount of chalcopyrite observed. Perhaps chalcopyrite is kinetically attracted to the pyrite-pyrrhotite grain boundary. It can never be stated for sure that pyrite is not in physical contact with the pyrrhotite because of the two dimensional nature of the thin section. This point becomes important when considering pyrite-pyrrhotite "equilibria" as will be discussed later in this paper. The pyrite grain is generally set in the anhedral pyrrhotite grain, but in most cases it is in direct contact with the surrounding silicates. In some large pyrrhotites, more than one euhedral pyrite grain is observed.

"Retrograde" Reaction Texture

Textural evidence suggests that a pyrrhotite --→ marcasite transformation has taken place to varying degrees in fifteen of the twenty-seven samples. Figure 7 is a photomicrograph of several pyrrhotite grains which have been altered to extremely fine-grained marcasite, and possibly pyrite (?), at the grain boundaries. This texture is not unlike the pyrrhotite, altering to marcasite, texture illustrated by Ramdohr (1969, Fig. 415). The photomicrograph shown in Figure 8 was taken from the same sample as Figure 7, and illustrates the completed pyrrhotite --→ marcasite reaction; no pyrrhotite remains. A somewhat curious pyrrhotite --→ marcasite is shown in Figure 9. Small,

Figure 7. "Retrograde" reaction. Photomicrograph of 80-28W, "spot" A - field of view is 300 x 200 microns. Anhedral pyrrhotite (white, cores of grains) is being replaced by extremely fine-grained marcasite (rims of grains). Straight edges of marcasite abutt against biotite cleavages.

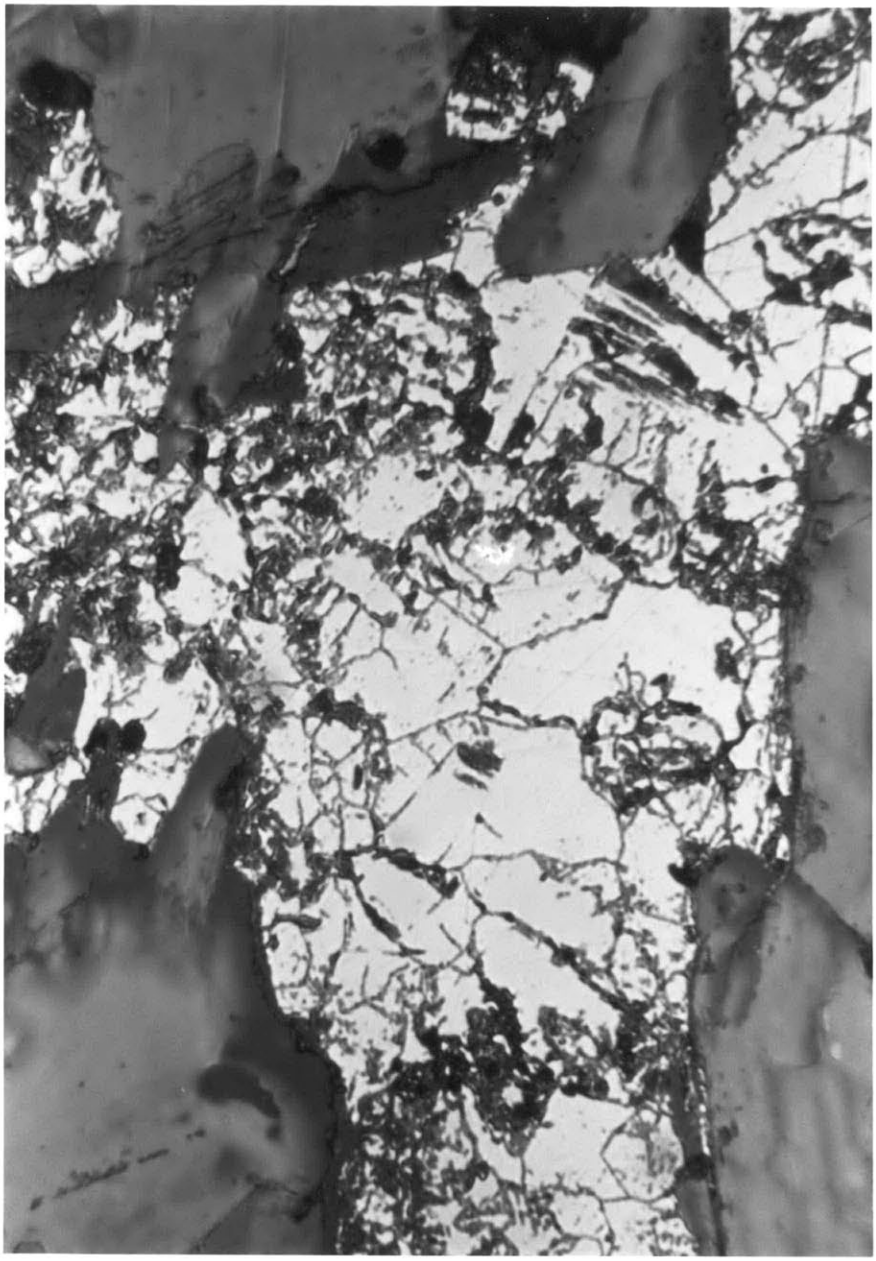

Figure 8. Completed "retrograde" reaction. Photomicrograph of sample 80-28W, "spot" B - field of view is 360 x 240 microns. Fine-grained marcasite with a few larger crystals visible.

Figure 9. "Balloon"-like "retrograde" reaction. Photomicrograph of sample 73-22E, "spot" X - field of view is 360 X 240 microns. "Balloons" of marcasite (basal cracks) in anhedral pyrrhotite grain (smooth). Note cracks connecting marcasite "balloons" to the edge of the pyrrhotite grain.

"balloon-like" patches of marcasite are situated inside the pyrrhotite grain. Upon careful examination, one can observe a small crack, with slight marcasite alteration, running from each of the marcasite "balloons" to the edge of the pyrrhotite grain! The cracks leading to the marcasite "balloons" strongly suggest that the pyrrhotite --→ marcasite involves the fluid phase. For some reason it must have been easier to transform the core of the pyrrhotite grain into marcasite, rather than the rim.

The pyrrhotite --→ marcasite transformation is most likely a retrograde reaction. Equilibration temperatures determined from pyrite-pyrrhotite pairs (discussed in Chapter VI) with substantial marcasite alteration are almost always much lower than the estimated peak metamorphic temperature. Interestingly enough, 80-28W ("spot" C), pictured in Figure 7, is the only major exception to this observation, despite approximately 50% pyrrhotite --→ marcasite alteration.

Both prograde and retrograde sulfide textures are often observed in the same iron sulfide grain, as is illustrated in Figure 10. This implies that pyrite (FeS_2) reacted to form pyrrhotite ($Fe_{1-x}S$), which in turn reacted to form marcasite (FeS_2). Of the fifteen samples that show pyrrhotite --→ marcasite alteration, thirteen also contain primary pyrite. This seems more than a coincidence when it is observed that of the twelve samples lacking marcasite, only five contain pyrite. The correlation between marcasite alteration of pyrrhotite and primary pyrite samples has important

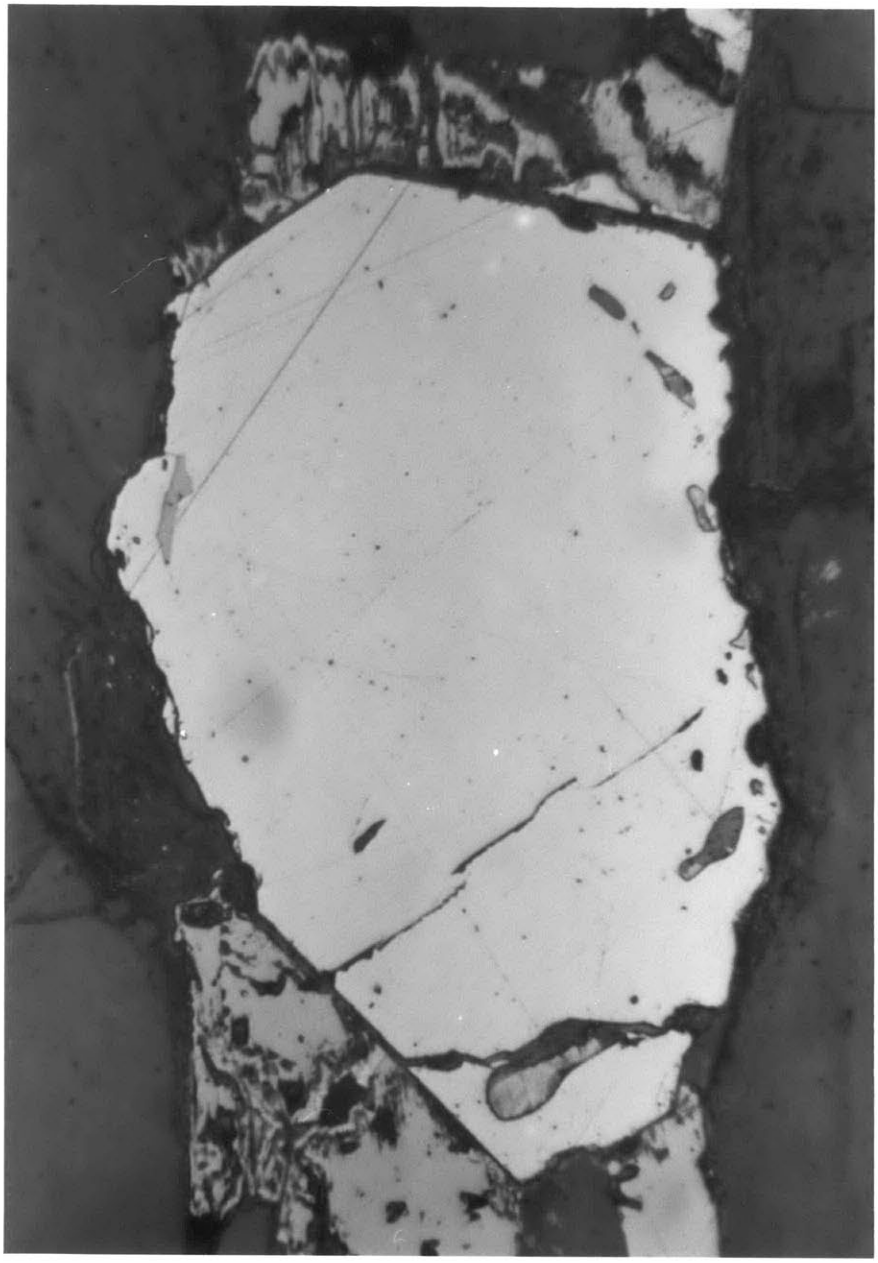

Figure 10. "Prograde" and "retrograde" reactions. Photomicrograph of sample 80-28W, "spot" A - field of view is 360 x 240 microns. Euhedral pyrite (light grey) in pyrrhotite grain (grey). A thin rim of marcasite (slightly lighter than pyrrhotite) surrounds pyrrhotite. A small anhedral grain of chalcopyrite can be seen along the pyrite-pyrrhotite border in the upper half of the figure.

implications for sulfur mobility which are discussed in Chapter VII. Marcasite is not observed in samples that lack pyrrhotite, and does not appear to be altering pyrite in any of the samples.

Secondary "Pyrite"

The New Berlin High School suite contains a complicated array of iron sulfide minerals. The paragenetic sequence for the sulfides in 80-70C (see Figure 11) is a good subject for debate. It will be proposed that the observed textures can be used as evidence for polymetamorphism.

Microprobe analyses reveal that all phases in Figure 11 are stoichiometric FeS_2 within the accuracy of the data. The euhedral, clean grain near the middle of the photomicrograph is thought to be primary pyrite. Unfortunately, microprobe analyses revealed no significant amounts of cobalt in the grain which would have helped back up this point. The phase in the lower half side of Figure 11, with abundant basal cracks and a "bird's eye" texture, closely resembles Figures 415 and 416 of Ramdohr (1969). The mineral exhibits moderately strong anisotropy which is consistent with Ramdohr's observations. Ramdohr believes the phase is an "intermediate product" that originates from pyrrhotite and would normally have altered to an extremely fine-grained aggregate of marcasite and pyrite. The upper half of the photomicrograph (Figure 11) is filled by a single grain of FeS_2 that is weakly anisotropic. This is thought to be

Figure 11. Secondary "pyrite". Photomicrograph of sample 80-70C, "spot" A - field of view is 1370 x 950 microns. Euhedral pyrite (white) with "intemediate product" of Ramdohr (1969) below, and secondary "pyrite" above. See text for explanation.

secondary "pyrite", which can be distinguished from the primary pyrite by its anhedral form, blebby (void) surface, slightly duller color, and magnetite inclusions. A planned x-ray study of secondary "pyrite" should reveal if the phase actually possesses the pyrite structure.

The following sequence of reactions is proposed for Figure 11: 1) Euhedral pyrite reacts to form pyrrhotite resulting in the typical prograde texture described above. The existence of pyrrhotite at some time in the sequence is demanded by the "bird's eye" structure which can not be formed directly from pyrite. The assemblage pyrite + pyrrhotite + secondary "pyrite" is seen in 80-70N. 2) Under retrograde conditions, the pyrrhotite is altered to the peculiar "intermediate product" instead of true marcasite for reasons unknown to myself; 3) The "intermediate product" was transformed into secondary "pyrite", possibly during a second, lower-grade, metamorphic event. Small amounts of magnetite are often present in fine-grained mixtures of marcasite and pyrite (Ramdohr, 1969) , so it is not inconsistent that the secondary pyrite developed small magnetite inclusions. The abundant voids on the polished surface of the secondary "pyrite" is considered evidence that pyrrhotite was an early "ancestor". Thus, the appearance of iron sulfides in the following order is deduced: pyrite --→ pyrrhotite (no longer present) --→ "intermediate product" ± marcasite --→ secondary "pyrite". The details of these reactions will be discussed later in Chapter VII.

The above-mentioned features that distinguished secondary "pyrite" and primary pyrite were used to determine if other samples in the suite contained secondary "pyrite". Three of the remaining five samples (80-70N, PP, and T) contain large grains, up to 1 mm across, of anhedral, blebby secondary "pyrite". In addition, all three samples contained clean, euhedral primary pyrite, along with pyrrhotite and marcasite, suggesting that a similar genetic sequence was common to all. The occurence of secondary "pyrite" in four of the six samples may be evidence for polymetamorphism of the New Berlin High School suite.

IV. MINERAL CHEMISTRY

Electron Microprobe - Equipment and Techniques

All microprobe analyses were performed on a three spectrometer MAC automated electron microprobe at the Massachusetts Institute of Technology. Analyses were made using a 15 kV accelerating voltage and a beam flag current of 60 nanoamps. The beam size was approximately 2 microns in diameter. All metal cations were analyzed with a LiF diffraction crystal; sulfur was done with a PET crystal. Counts were made for twenty seconds or 100,000 counts. On-line matrix corrections were made using a ZAF routine on a Tracor Northern TN-2000 microcumputer.

The sulfide standards used are listed in Appendix I. Synthetic pyrrhotite and troilite were used as working standards to check the Fe and S standardizations every several hours or whenever totals deviated from 100 %. The elements routinely analyzed for were as follows: Pyrrhotite - Fe and S; Pyrite and polymorphs - Co, Fe, and S; Chalcopyrite - Cu, Fe, and S; Pentlandite - Cu, Ni, Fe, and S. In some of the later analyses, the amount of Co in selected pyrite grains was estimated by counting on the peak for 20 seconds. Numerous checks were made for trace amounts of Co, Ni, Cu, and Zn. The sum total of these minor elements never exceeded 1.0% except for Ni in one pyrrhotite grain (see "Pyrrhotite" below).

In order to obtain accurate data for pyrite-pyrrhotite equilibrium analysis, the acceptable totals for pyrrhotite

analyses were set at 99.50 to 100.50. In a few cases, when the filament was unstable, the acceptable range was relaxed to 99.00 to 101.00. Pyrite totals were typically in the range 100.50 to 101.50, while chalcopyrite totals were generally between 98.50 and 99.50. The reasons for the pyrite and chalcopyrite totals not being closer to 100.00 are not clear. It is suggested that the use of pyrrhotite for the Fe standard resulted in a systematic error for pyrite and chalcopyrite analyses because of their substantially lower Fe contents. Checks for the presence of minor elements (Ni, Cu, Co, and Zn) were made whenever totals fell below the typical range for the mineral.

Approximate errors for microprobe analyses are difficult to estimate. Analyses of pyrrhotite are thought to be accurate to $\pm$0.25 weight percent Fe and S (perhaps only as good as $\pm$ 0.50 wt %), since a pyrrhotite standard was used and totals were usually in the range of 99.50 to 100.50. Pyrite and chalcopyrite analyses are believed to be less accurate - $\pm$ 1 wt % for each element.

Just under 1000 sulfide analyses were obtained using the electron microprobe. Points judged to be anomalous were re-analyzed with the usual result that the "anomaly" dissappeared. The number of analyses per grain varied proportionately with the interest in the mineral and grain size - Pyrrhotite, 3 to 10 in early days, increasing later to 5 to 15; Pyrite and marcasite, 3 to 7; and Chalcopyrite, 2 to 3 owing to its small grain size. Figure 12 illustrates the

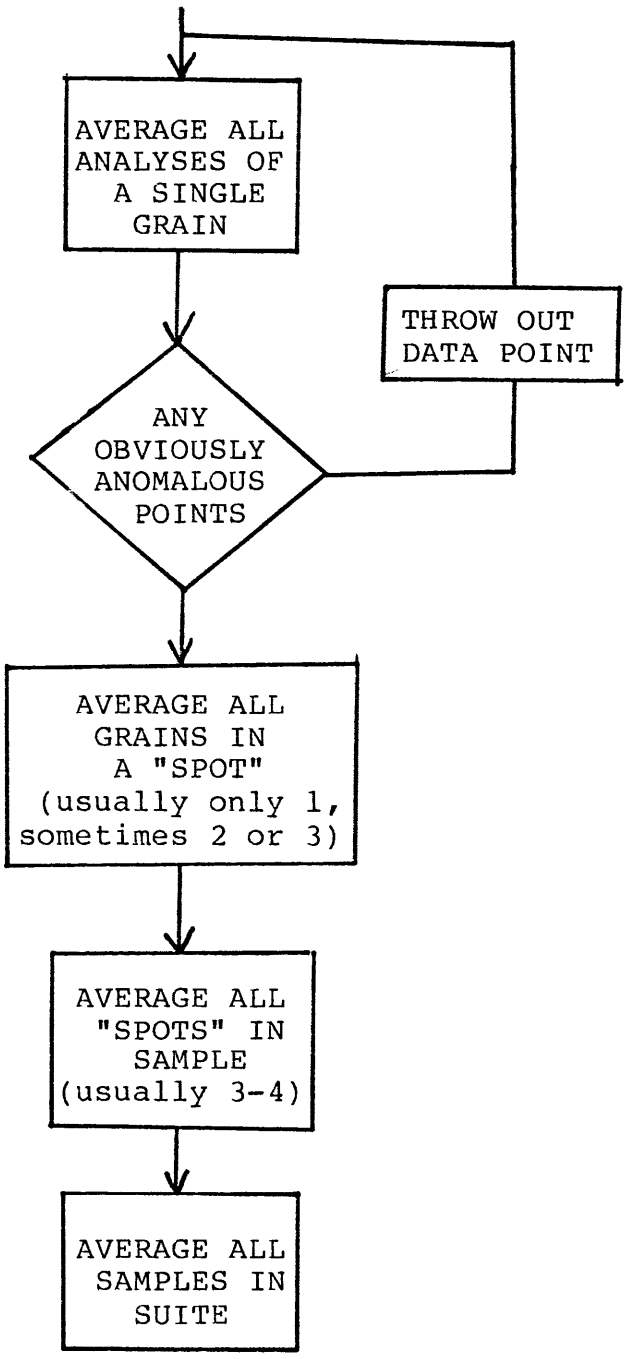

Figure 12. Method used to average electron microprobe analyses.

method that was used to arrive at various "averages". In this manner, grains with fewer analyses than others were not unfairly biased.

Electron Microprobe - Results

Microprobe analyses for all sulfide phases are tabulated in Appendix II.

Pyrrhotite. The deviation from stoichiometric FeS, "x" in $Fe_{1-x}S$, varied from 0.86 to 0.92 in this study. Another measure of non-stoichiometry is N_{FeS}, the mole fraction of FeS in the system FeS-S_2, which can be expressed algebraically as:

$$N_{FeS} = \frac{FeS}{FeS + S_2} = \frac{2Fe}{Fe + S}$$

N_{FeS} values for individual pyrrhotite grains range from 0.922 (77-58D, "spot" C) to 0.959 (80-70PP, "spot" D). N_{FeS} values for pyrrhotites in all samples are tabulated in Appendix II. Average pyrrhotite compositions for pyrite-pyrrhotite "spots" within a sample are given as well as sample averages.

The presence of other elements, aside from Fe and S, was checked whenever the microprobe totals fell below 99.50. The sum total weight percent of Cu, Ni, Zn, and Co in pyrrhotite never exceeded 0.75 %, except in 77-18X1, where the pyrrhotite analyzed contained an average nickel concentration of 2.61 weight percent. Sample 77-18X1 also contains pentlandite, thus it is not surprising that the pyrrhotite contains an abnormal amount of nickel. Small amounts of various metals can substitute for Fe in pyrrhotite, but this

amount of nickel is probably present as pentlandite impurity (Deer et al., p.451). The mole fraction of FeS in the system FeS-S_2 was recalculated for 77-18X1 by assuming all nickel in the analysis to be $(Fe_{3.4}Ni_{5.6})S_8$ - the average pentlandite composition for the sample.

No Fe:S zoning was observed in individual pyrrhotite grains, with the one exception of 73-22E ("spot" C) where a distinct band of Fe-rich pyrrhotite (N=0.943) cuts across an otherwise unzoned grain (N=0.933). Cracks with evidence of sulfide dissolution are seen elsewhere in the sample, though none are seen at this particular "spot". It seems likely, however, that the Fe-rich band is associated with a crack, but the two-dimensional nature of the thin section prevents the actual observation of the crack.

Pyrrhotite compositions within a sample exhibit a systematic variation according to the presence or absence of pyrite. For a given sample, pyrrhotite N_{FeS} values are an average of .003 higher for pyrite-bearing "spots" as compared to pyrite-absent "spots". The range in ΔN_{FeS} is 0 to +0.006, and is never negative. This contradicts the studies of Toulmin and Barton (1964) which show that for a given temperature, the N_{FeS} value for pyrrhotite should be lower when pyrite is present. An interesting explanation for this phenomenon is proposed in Chapter VII.

There does not appear to be any systematic variation in the average pyrrhotite composition with increasing metamorphic grade. However, there does appear to be a general decrease in

pyrrhotite Fe-content with increasing metamorphic grade for pyrite-bearing "spots". This is predicted by pyrite-pyrrhotite equilibria studies and will be discussed in Chapter VI.

Pyrite. Microprobe analyses of pyrite yield formulas that are stoichiometric FeS_2 within the accuracy of the analyses (see Appendix II). Significant deviations from stoichiometry are generally the result of high cation total which can usually be attributed to the sulfur peak having drifted. Cobalt is the only element that appears to substitute for iron in significant amounts; spot checks indicate that the combined weight percent of other metals in pyrite is less than 0.50 %.

Average pyrite compositions show a range in $CoFe_{-1}$ substitution from 0.00 up to 2.50 wt %. Individual pyrite grains are often zoned with respect to cobalt content. Analyses from sample 77-58D ("spot" A) range from a high of 4.58 wt % cobalt near the center to 1.01 wt % cobalt near the rim. Similar core to rim zoning is seen in other pyrites from different samples. It is interesting to note that appreciable cobalt substitution ($CoFe_{-1}$ > 0.010 mole percent) is only observed in pyrite grains coexisting with pyrrhotite. However, not all pyrites that touch pyrrhotite contain cobalt. It seems reasonable that the the pyrite --→ pyrrhotite reaction will concentrate cobalt in the pyrite (since cobalt is unstable in the pyrrhotite lattice), but the zoning profile can not be explained. In any case, samples with a zoned pyrite grain must have cooled relatively quickly in order for

the grain not to have been homogenized via cobalt diffusion.

Marcasite and other FeS_2 polymorphs. Microprobe analyses reveal no reason not to believe that marcasite is stoichiometric FeS_2 (see Appendix II). It is common to get poor totals when analyzing marcasite because of its poor polishing characteristics (owing to the extremely fine grain size). Very small amounts of cobalt may be present in marcasite by weight, though this value is well within the accuracy of the microprobe analyses.

The other FeS_2 phases encountered in this study - secondary "pyrite" and the so-called "intermediate product" - are also stoichiometric FeS_2 within the accuracy of the data.

Chalcopyrite. Chalcopyrite analyses proved to be somewhat of an enigma. While always close to the ideal $CuFeS_2$ formula, the iron to copper ratio is consistently greater than unity (Appendix II shows that only 3 grains out of the 43 analyzed show Fe<Cu). This deviation from the ideal 1:1 ratio may be real, or it could be the result of the chalcopyrite standard being inaccurate. Unlike Fe and S, no working standards were used to monitor the Cu standardization - only if totals were unusually low was the Cu re-standardized.

The sum total of metal cations other than Cu and Fe, was determined by spot checks to be always less than 0.75 weight percent. Zinc was usually the most abundant of these minor elements. No systematic variation in chalcopyrite analyses with metamorphic grade or sulfide assemblage is

observed.

Pentlandite. Three analyses of a single pentlandite grain in 77-18X1 reveal its formula to be $(Fe_{3.41}Ni_{5.58}Cu_{0.13})S_8$. This is reasonably close to $(Fe,Ni)_9S_8$ - the idealized formula.

V. DOCUMENTATION OF PYRITE-PYRRHOTITE TRANSITION

The transformation of pyrite to pyrrhotite during prograde metamorphism has been well-documented in metamorphosed sediments. Excellent literature reviews of the mineralogical changes observed in iron sulfides in metasediments are provided by McDonald (1967) and Ferry (1981). Much less is known about the behavior of iron sulfides in metamorphosed volcanics. A review of the recent literature reveals that the same phenomenon observed in metasediments may be present in metavolcanics; pyrite being the dominant iron sulfide in unmetamorphosed or weakly metamorphosed mafic and felsic volcanics, while pyrrhotite becoming more abundant at higher metamorphic grades.

Pyrite in Volcanic Rocks

Sillitoe (1973) discussed the nature of Cyprus and Kuroko-type ore deposits, both of which are formed in subaqueous volcanic environments. Cyprus ores consist largely of pyrite, with less sphalerite, and subordinate chalcopyrite. These ore bodies are overlain by iron oxide-rich mudstones and underlain by pyritic stockworks representing hydrothermal conduits. Kuroko ore deposits contain pyrite and chalcopyrite bands intermixed with basaltic layers. The presence of pyrrhotite is not reported in either environment.

Williams *et al.* (1977) studied the Planes-San Antonio pyritic deposit of Rio Tinto, Spain. The sedimentary-

volcanogenic deposit is believed to have been precipitated as a chemical sediment from sea-floor hot springs in an environment not unlike that of the Ammonoosuc Volcanics. The hot springs were associated with the Lower Carboniferous volcanic arc of southwest Iberia. The ore deposit was laid down during the late stages of arc evolution within the waning episodes of submarine explosive volcanism. Pyrite, chalcopyrite, sphalerite, and galena are the dominant sulfides in the ore body. No pyrrhotite is observed.

The effect of low-grade oxidative diagenesis on layer 2 oceanic basalts was studied by Andrews (1979). He concluded that any pyrrhotite that may be present in freshly deposited submarine volcanics will be quickly transformed into pyrite through sea-water interaction. Ramdohr (1969) concluded that "only transitional members of subvolcanic epithermal deposits contain pyrrhotite, while typical deposits do not".

A regional study of pyrite deposits in the Ural Moutains by Zavaritsky (1950) confirms the lack of pyrrhotite in unmetamorphosed volcanics. The sulfide ore deposits occur in Siluro-Devonian volcanic rocks which have been altered to greenstones and greenschists in the Variscan Orogeny. The unmetamorphosed deposits in the Southern Urals contain pyrite, marcasite, melnikovite, and "an earthy variety of FeS_2 associated with the melnikovite". Chalcopyrite, sphalerite, and wurtzite are also present. In some of the Southern Ural deposits, colloform textures of pyrite are observed replacing marcasite and melnikovite. In the Middle Urals, the pyritic

deposits have been deformed by general "dynamic" metamorphism. Pyrite grains have been mechanically deformed, while chalcopyrite and sphalerite grains, being softer, behaved ductily. Poorly preserved pyrite colloform textures are locally present. Pyrite is the only iron sulfide observed in these deposits with the one exception of the San-Donato deposit. This pyritic deposit was cut by a pre-metamorphic, andesitic-porphyry dike. At the contact pyrite was transformed to pyrrhotite. With the later dynamic metamorphism, some of the pyrrhotite reacted to form pyrite and magnetite. The formation of magnetite suugests that sulfur may be removed from the system at high temperatures. It is also possible that at high temperatures iron was drawn from the surrounding silicates, while at lower temperatures, it was not possible reverse the reaction, thus pyrrhotite formed pyrite and magnetite.

Thus, from studies of subaqueous volcanic environments in the literature, I conclude that all or almost all iron sulfide in submarine volcanics is pyrite (or will be after low-grade diagenesis).

Pyrite and Pyrrhotite in Metavolcanics

The conversion of pyrite to pyrrhotite with increasing metamorphic grade has been demonstrated in metavolcanics by several workers.

The effects of regional metamorphism on strata-bound pyritic base-metal sulfide deposits in Norway has been studied

by Vokes (1968). The ore deposits are exposed in a 1500 km long Paleozoic geosynclinal belt in Norway and adjacent Sweden. The sulfide ores occur in greenstones, greenschists, amphibolites, phyllites, and mica schists. Lower greenschist to almandine-amphibolite facies metamorphism was imposed on the deposits in the Caledonian Orogeny. Vokes believes that the ore deposits are genetically related to the Caledonian Orogeny, but were emplaced prior to the culmination of the orogeny.

Vokes concluded that "the increasing frequency of pyrrhotite in the ores at higher-grade areas strongly suggests that pyrrhotite may be of metamorphic origin". However, he could not construct a "sulfide mineral facies" similar to the silicate metamorphic facies, thereby implying that he did not observe a clean pyrite --→ pyrrhotite "isograd". Vokes proposed two explanations for the lack of sulfide mineral facies - 1) the large stability fields of the common sulfide minerals, and 2) the relatively simple chemical composition of the sulfide masses.

The sulfide ore deposits in the metamorphic terrains of Japan heve been studied by Kanehira and Tatsumi (1970). They summarized the features of bedded cupriferous iron sulfide deposits in various areas of Japan similar to the Sanbagwa metamorphic terrain. Their findings were: 1) The deposits occur in the geosynclinal pile - many are associated with basic volcanics (and their metamorphosed equivalents), while some are associated with acidic or intermediate volcanics.

2) The ore bodies are tabular or lens-shaped and in general conformable. 3) The grain size of the sulfides increases from unmetamorphosed and low-grade rocks to high-grade rocks. 4) Colloform textures are common in the unmetamorphosed and weakly metamorphosed terrains, and are considered to be relict textures of the original sulfide ores. 5) Ores in unmetamorphosed and weakly metamorphosed terrains consist of pyrite and chalcopyrite with lesser amounts of sphalerite and gangue. At higher metamorphic grades, pyrrhotite becomes considerably more abundant, as is demonstrated in the Honko ore zone of the Hitachi mine.

Bachinski (1976) studied the effects of thermal metamorphism on the cupriferous iron sulfide deposits of Notre Dame Bay, Newfoundland. The sulfide ore deposits occur in mafic volcanics interpreted to be ophiolites. The ore deposits are thought to have been formed in either layer 2 oceanic crust, or at the sea water/layer 2 pillow basalt interface. Thermal metamorphism has transformed low-grade greenschist (chlorite zone) rocks into hornblende-hornfels facies rocks. Ores in the greenschist facies contain predominantly pyrite, while hornblende-hornfel deposits consist of pyrrhotite and magnetite. Chlorites in the greenschist zone are iron-rich with the most iron-rich chlorites occurring in the ore zone itself. Fe-Mg silicates in the hornblende hornfels are Mg-rich and become less Mg-rich (more Fe-rich) near the edges of the ore zone. Bachinski (1976) concluded that iron is removed from the silicates via a

reaction with pyrite. He believes that pyrite reacts to form pyrrhotite by losing sulfur, but that the sulfur is not lost from the system. Instead, the sulfur released draws iron from the surrounding silicates to form more pyrrhotite.

The behavior of iron-sulfides in metavolcanics outside of ore bodies has only been reported from Japan. Banno and Kanehira (1961) have documented a pyrite --→ pyrrhotite transition with increasing metamorphic grade in the Central Abukuma Terrane. Sulfides did not exceed 0.5 % by volume in the samples studied. Of the three sulfide-bearing samples they collected from the greenschist facies (Zone A), all contained pyrite and no pyrrhotite. Of the eleven amphibolite-facies (Zones B and C) samples, none contained pyrite and all contained pyrrhotite. Banno and Kinehira also studied the ore deposits in the Bessi district where the pyrite --→ pyrrhotite transition is not as well-demonstrated. This may be the result of the metamorphic grades studied (glaucophane facies to epidote-amphibolite facies). They concluded that pyrite was stable in basic schists in the greenschist and epidote-amphibolite zones, while pyrrhotite became stable in the upper greenschist zone and remained stable up to the end of the amphibolite zone. The common occurence of pyrite and pyrrhotite in equilibrium led Banno and Kanehira to suggest that sulfur was inert and that the sulfur and iron contents of the rocks were determined before regional metamorphism took place.

The above study was extended by Kanehira and others

(1964) to include several additional metamorphic terrains. No pyrite --→ pyrrhotite transition could be documented in the three terrains for which complete data was presented (not including the two terrains mentioned above).

In summary, literature studies indicate that a pyrite --→ pyrrhotite transition occurs with increasing metamorphic grade in volcanic sulfide ore deposits. The same transition in rocks containing less than 5 % disseminated sulfides is well documented in only one of five Japanese metamorphic terrains. The rocks studied by Banno and Kanehira (1961) and Kanehira and others (1964) were from paired metamorphic belts, and therefore underwent a substantially different P-T history than the regionally metamorphosed Ammonoosuc Volcanics.

Pyrite-Pyrrhotite Transition in the Ammonoosuc Volcanics

The modal abundances of pyrite and pyrrhotite were estimated for 152 samples, in order to document the pyrite to pyrrhotite transition observed with increasing metamorphic grade in the Ammonoosuc Volcanics. The amount of each sulfide phase was classified as either rare, common, or abundant. Boundaries were set for each category as follows: rare, < 0.2 modal percent; common, ≥ 0.2 % and < 2.0 %; abundant, > 2.0 %. Point counting of five samples (2500 points each) resulted in "standards" against which a sample could be compared if the modal percent of a sulfide phase was close to one of the boundaries. Products of retrograde or surface conditions were counted as representing the primary sulfide that they were

replacing - marcasite as pyrrhotite, and limonite usually as pyrite.

Samples for modal analysis were chosen from all samples from a given suite, not just those analyzed with the electron micrprobe. In this manner, the data was not skewed towards pyrrhotite-bearing samples. At least 15 samples were analyzed from each suite, except for the Wilder Dam suite which only contains a total of twelve samples. In addition to the seven suites for which polished thin-sections were available, seven polished slabs were made from the I-91 low-grade suite. Sulfide modal abundances were estimated for this additional suite in order to increase the range in estimated metamorphic grade.

Each modal percent category was assigned a value: rare = 1, common = 2, and abundant = 3. The sum of these values was calculated for each sulfide phase in the eight suites. The estimated sulfide modal abundances for all 152 samples, including totals by suite, are tabulated in Appendix III.

The amount of pyrite vs. pyrrhotite in a suite can be estimated from the "abundance" totals calculated for each suite. The ratio pyrite to (pyrite + pyrrhotite), or simply py/py+po, was calculated for each suite and plotted as a function of increasing metamorphic grade in Figure 13. A suite containing pyrite and no pyrrhotite would plot at py/py+po = 1.0, while a suite with pyrrhotite and no pyrite plots at 0.0. The estimated error in py/py+po for each suite

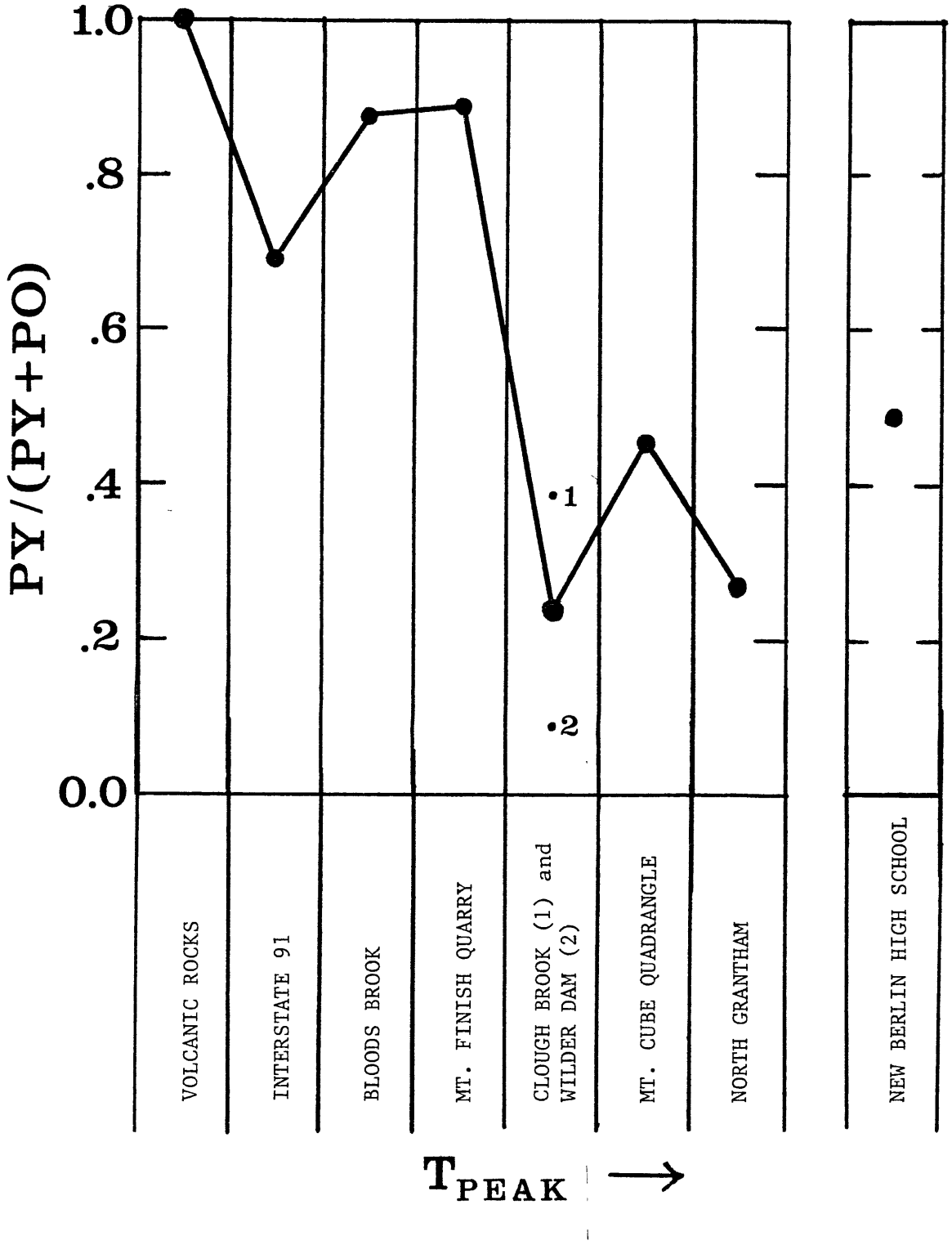

Figure 13. Plot of py/py+po (reaction progress) vs. increasing metamorphic grade. Modal abundances were estimated from a minimum of fifteen samples for each suite (except Wilder Dam which only has 12). Estimated error in py/py+po is ~0.02.

is probably $\pm$0.2. This error could be reduced by doing detailed point counting, but the overall results would not be significantly improved.

Figure 13 clearly demonstrates that the amount of pyrite versus pyrrhotite in a suite generally decreases with increasing metamorphic grade. This strongly suggests that pyrite is transformed to pyrrhotite during regional metamorphism, and that the progress of the reaction is favored by increasing metamorphic grade. Pyrrhotite without pyrite is observed in the four highest-grade suites. (The two pyrrhotite-bearing samples in I-91 are leucocratic, in contrast to the rest of the suite, and probably represent sulfides deposited in a late-stage hydrothermal vein.) The presence of pyrrhotite without pyrite at higher metamorphic grades, further supports the idea that the pyrite --→ pyrrhotite reaction is favored by increaaesing metamorphic grade.

Figure 13 and Appendix III also show that the pyrite --→ pyrrhotite transition can not be mapped as a clean "isograd" in the Ammonoosuc Volcanics. Pyrite and pyrrhotite are observed in all eight suites, though the py/py+po ratio generally decreases with increasing metamorphic grade. The amount of pyrite that has been transformed to pyrrhotite varies considerably within a given suite. Samples containing pyrite with no pyrrhotite, indicating that the reaction hasn't even started, are observed in all suites, except for Wilder Dam. This strongly suggests that temperature (metamorphic

grade) is not the only controlling factor in the pyrite --→ pyrrhotite reaction.

The New Berlin High School suite yields a py/py+po ratio of 0.485. This ratio is roughly "equivalent" to the py/py+po ratios of the Clough Brook and Mt. Cube suites. This cannot be used as an estimate of metamorphic grade for the New Berlin High School suite, because it implicitly assumes that the py/py+po ratio is only a function of metamorphic grade, which is clearly invalid. In addition, the possibility of polymetamorphism for the suite makes any estimate of metamorphic grade from pyrite-pyrrhotite abundances highly suspect.

In conlusion, the transformation of pyrite --→ pyrrhotite with increasing metamorphic grade can be documented in the Ammonoosuc Volcanics. The wide range in pyrite vs. pyrrhotite seen in each suite strongly suggests that the reaction is not controlled solely by metamorphic grade.

VI. PYRITE-PYRRHOTITE EQUILIBRIA

The Pyrite-Pyrrhotite Geothermometer

Many workers have investigated the phase relations in the system Fe-S (e.g.Hansen and Anderko, 1958; Kullerud and Yoder, 1959). Figure 14 shows the binary phase diagram for the Fe-S system. The pyrite-pyrrhotite solvus was determined experimentally by Arnold (1962) and is shown in Figure 15. The experimentally determined change in pyrrhotite composition with increasing temperature in equilibrium with pyrite suggests that the coexistence of pyrrhotite and pyrite could be used as a geothermometer.

In order to discuss the pyrite-pyrrhotite geothermometer in terms of thermodynamics, the system components need to be defined. For reasons of simplicity, FeS and S_2 were chosen as the system components. The equilibrium coexistence of pyrite + pyrrhotite + sulfur-rich fluid will define a divariant plane in P-T-f(S_2) space. This can be seen by solving the phase rule, $F = C - \phi + V$, where F is the degrees of freedom, C is the number of system components (two), ϕ is the number of phases (three), and V is the number of external varibles imposed on the system (three - pressure, temperature, and sulfur fugacity). The effects of pressure are negligible for $P < 2$ kilobars (Arnold, 1962), so that the plane becomes a univariant curve in T-f(S_2) space. Since pyrrhotite is non-stoichiometric ($Fe_{1-x}S$), with the Fe:S ratio varying with the sulfur fugacity, knowledge of the pyrrhotite composition

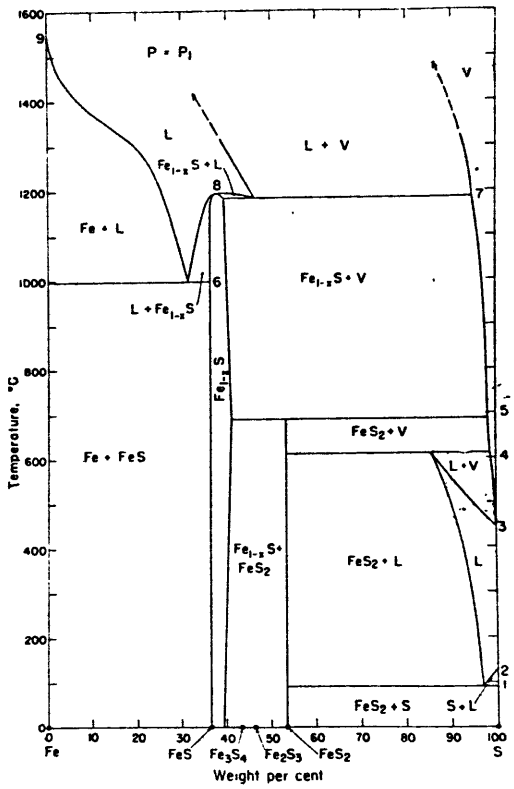

Figure 14. Fe-S binary phase diagram (taken from Kullerud and Yoder, 1959)

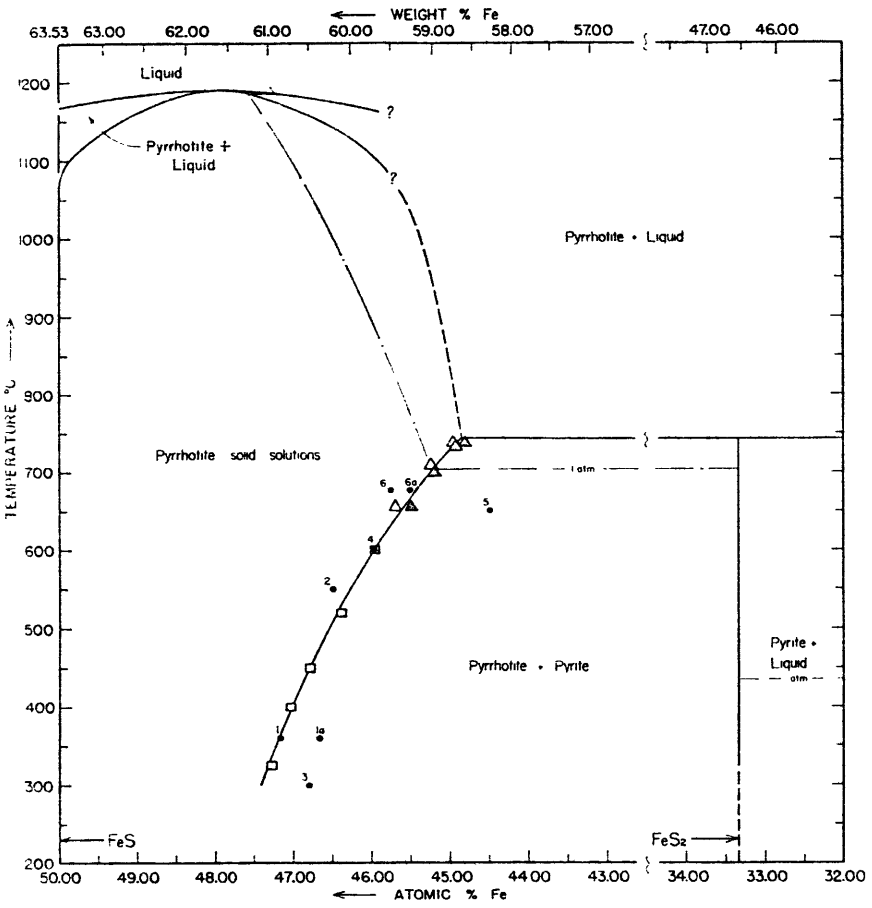

Figure 15. Experimentally determined pyrite-pyrrhotite solvus (taken from Arnold, 1962).

will define the sulfur fugacity and thus the temperature at which the pyrite and pyrrhotite equilibrated. For a more thermodynamically rigorous treatment of pyrite-pyrrhotite equilibrium the reader is referred to excellent articles by Toulmin and Barton (1964) and Froese and Gunter (1976).

Toulmin and Barton (1964) used the electrum-tarnish method to accurately determine the $f(S_2)$ vs. T curve for the univariant assemblage pyrite + pyrrhotite + sulfur-fluid from 743 to 325°C (see Figure 16). Points lying on this curve are tabulated in Appendix IV. Toulmin and Barton's determination of the pyrrhotite composition in equilibrium with pyrite agrees well with the results of Arnold (1962). Their experimentally determined pyrrhotite solvus may be used to estimate temperatures of formation and sulfur fugacities of natural pyrite-pyrrhotite assemblages if certain assumptions can be made. The assumptions that must be made to use pyrite-pyrrhotite equilibrium as a metamorphic geothermometer are: (1) that the pyrite and pyrrhotite were in equilibrium with each other at the peak of metamorphism, (2) that the equilibrium pyrrhotite composition has not changed significantly during retrograde metamorphism or subsequent geologic events, and (3) that small concentrations of trace elements, such as Ni and Cu, do not significantly affect the equilibrium relations. The above assumptions are common to all metamorphic geothermometers.

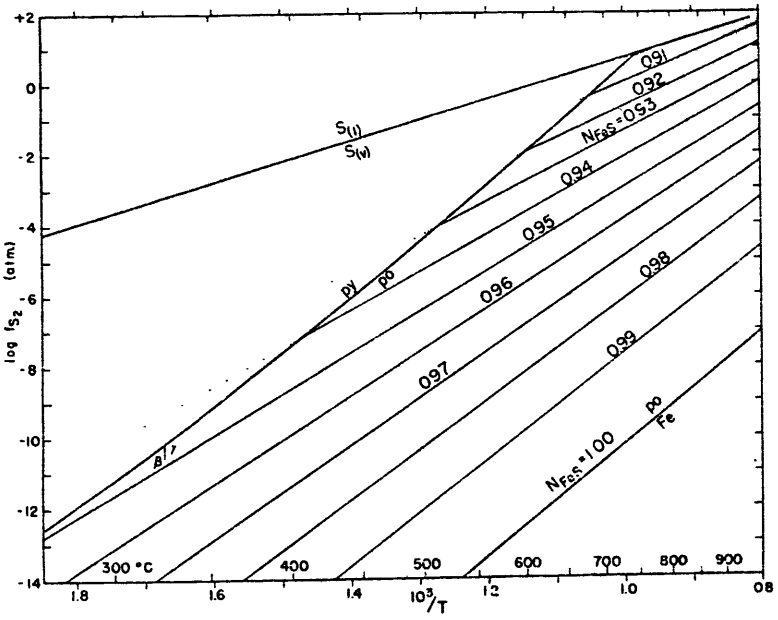

Figure 16. Log f(S_2) vs. T diagram with pyrite-pyrrhotite equilibrium curve (taken from Toulmin and Barton, 1964).

Pyrite-Pyrrhotite Geothermometry in Natural Rocks

Arnold (1962) analyzed pyrrhotites by the X-ray spacing method in ten pyrrhotite-pyrite assemblages from hydrothermal type ore deposits. The estimated temperatures of crystallization ranged from 425° to 520°C. The confining pressure was assumed to be 2000 bars, hence no correction for pressure was necessary. In four of the samples, the iron content in sphalerite was measured by standard wet chemical methods. Temperature estimates (uncorrected for pressure) determined from the sphalerite compositions agreed excellently with the pyrrhotite data. When the sphalerite temperature estimates were corrected for a confining pressure of 2000 bars, the sphalerite temperatures exceeded the pyrrhotite temperatures by an average of 40°C. Arnold (1962) concluded that the temperature discrepancies were within the range of experimental error, and that the temperature estimates were in good agreement at the assumed pressure.

Schreyer et al. (1964) determined temperatures of 250-350°C for the Silderberg ore deposit in Germany from pyrrhotites coexisting with pyrite. These values were considerably lower than those deduced from the sphalerite geothermometer in the same ore. The authors attributed the discrepancy to re-equilibration of pyrite + pyrrhotite at lower temperatures during retrograde metamorphism. They were uncertain, however, as to whether the lower pyrrhotite temperatures were the result of a particular event in later geologic history or plain re-equilibration during the cooling

of the deposit. Vokes (1968) attempted to use the pyrite-pyrrhotite geothermometer to indicate peak metamorphic temperatures for the sulfide ore deposits in Norway and met with a similar lack of success - rather, the pyrite + pyrrhotite seemed to have re-equilibrated under retrograde conditions at quite low temperatures.

The phase relations of pyrrhotite were investigated by Desborough and Carpenter (1965), with the result that three structural types of pyrrhotite were distinguished. Heaxagonal pyrrhotite (a=2A,7C) was found to be stable above 315±10°C, while monoclinic - Fe_7S_8 (2B,4C) and hexagonal forms (2A,5C) were found to be stable below 315°C. They concluded from their studies that "numerous processes may lead to the development of pyrrhotite of pyrrhotite and pyrite-pyrrhotite assemblages in ore deposits and that the composition of pyrrhotite associated with pyrite may be <u>completely meaningless</u> in terms of geothermometry". The "numerous processes" postulated for monoclinic (Fe_7S_8) pyrrhotite formation include quenching, very slow cooling, oxidation, hydrothermal modification, and direct pyrrhotite formation. It was demonstrated that Fe_7S_8 can form at temperatures as high as 600°C (under high oxygen pressures), and as low as 130°C (interaction with sulfide-rich fluids). In view of these considerations, they concluded that monoclinic pyrrhotite is essentially of no value as a geothermometer. In addition, Desborough and Carpeneter criticized the extrapolation of the pyrrhotite-pyrite solvus down to 200°C

(by Toulmin and Barton, 1964) as being unjustified in light of the pyrrhotite phase transformation encountered at 315°C.

Guidotti (1970) analyzed pyrrhotites in four pyrite + pyrrhotite-bearing metapelites in the sillimanite zone from the Oquossoc area, Maine. The four samples yielded temperatures ranging between 200° and 310°C, considerably lower than temperatures expected for the sillimanite zone. Clearly, the pyrite + pyrrhotite reached a new equilibrium at some temperature below the metamorphic peak. Guidotti concluded that the apparently strong tendency of pyrrhotite to re-equilibrate to new compositions as the temperature decreases in regionally metamorphosed terrains precludes the use of the pyrite-pyrrhotite geothermometer. The same phenomenon was observed by Ferry (1981) in the graphitic sulfide-rich schists of south-central Maine.

Attempts at applying pyrite-pyrrhotite geothermometry to natural assemblages appear to be plagued by the re-equilibration of pyrrhotite under retrograde conditions. The tendency of pyrrhotite to re-equilibrate at temperatures lower than the metamorphic peak is confirmed by my investigation of pyrite-pyrrhotite equilibria in the Ammonoosuc Volcanics discussed below.

Pyrite-Pyrrhotite Geothermometry in the Ammonoosuc Volcanics

Eighteen of the twenty-seven samples analyzed with the electron microprobe contain pyrrhotite and pyrite. It was found that the average composition of a pyrrhotite grain

yielded higher temperatures than a pyrrhotite analysis taken right next to the pyrite grain. This suggests that local retrograde re-equilibration must of taken place at the boundary, thus average pyrrhotite grain compositions were used for geothermometry calculations. If microprobe analyses of pyrrhotite are accurate to within $\pm$ 0.25 weight percent in Fe and S, then values for N_{FeS} are accurate to $\pm$0.003. This leads to an estimated error of $\pm$30°C for temperatures calculated from pyrite-pyrrhotite equilibria. Average pyrrhotite compositions for each sample, along with the calculated temperatures and sulfur fugacities are tabulated in Table 4. The data for the pyrite-pyrrhotite "spot" yielding the highest temperature (lowest N_{FeS}) within each sample are tabulated in Table 5. Appendix III contains complete pyrite-pyrrhotite geothermometry data for all "spots" in the eighteen samples. It should be noted that Tables 4 and 5 as well as Appendix III are not corrected for pressure. Arnold (1962) determined that the effect of pressure on the geothermometer was within the experimental error in measuring the pyrrhotite composition for pressures less than 2 kilobars. For typical regional metamorphic pressures (~4 to 5 kilobars), however, the neglecting of pressure may not be valid, as will be discussed in more detail below. In any case, it will be assumed that pressure effects are negligible in the following discussion.

Bloods Brook. Only one sample contains pyrite and pyrrhotite in the the Bloods Brook suite. The temperature calculated

SAMPLE #	# OF SPOTS	$\overline{N}_{FeS}$	EST. T_{PEAK} (°C)	CALC. T(°C)	CALC. LOG $f(S_2)$
Bloods Brook					
77-23D	1	0.935	465°	450°	-5.78
Mt. Finish					
77-15Y	3	0.936	480°	450°	-5.78
Clough Brook					
77-18M	1	0.944	510°	354°	-9.00
77-18X1	1	0.935	510°	461°	-5.47
Mt. Cube Quad					
73-22E	1	0.932	535°	492°	-4.72
73-25A	2	0.9315	535°	497°	-4.46
73-25B *	1	0.938	535°	428°	-6.46
73-27C	1	0.931	535°	502°	-4.32
73-31B *	2	0.935	535°	461°	-5.47
77-58D	4	0.930	535°	512°	-4.05
AVERAGE	(6)	0.933	535°	482°	-4.86
AVG(w/o *)	(4)	0.931	535°	502°	-4.32
North Grantham					
80-28W	2	0.934	575°	472°	-5.16
New Berlin HS					
80-70C	1	0.942	?	378°	-8.13
80-70J	2	0.939	?	417°	-6.82
80-70K	1	0.945	?	341°	-9.53
80-70N	1	0.939	?	417°	-6.82
80-70PP	3	0.956	?	<300°	-
80-70T	2	0.940	?	404°	-7.22
AVG(w/o PP)	(5)	0.941	?	391°	-7.68
AVG(w/o PP,K)	(4)	0.940	?	404°	-7.22

Table 4. Average temperatures and sulfur fugacities as determined from pyrite-pyrrhotite analyses.

SAMPLE #	"SPOT"	$\bar{N}_{FeS}$	EST. T_{PEAK} (°C)	CALC. T (°C)	CALC. LOG f(S2)
Bloods Brook					
77-23D	C	0.936	465°	450°	-5.78
Mt. Finish					
77-15Y	B	0.931	480°	502°	-4.32
Clough Brook					
77-18M	A	0.944	510°	354°	-9.00
77-18X1	A	0.935	510°	461°	-5.47
Mt. Cube Quad					
73-22E	B	0.932	535°	492°	-4.59
73-25A	B	0.931	535°	502°	-4.32
73-25B	A	0.938	535°	428°	-6.46
73-27C	C	0.931	535°	502°	-4.32
73-31B	B	0.933	535°	482°	-4.86
77-58D	C	0.922	535°	583°	-2.36
AVERAGE	(6)	0.931	535°	502°	-4.32
North Grantham					
80-28W	C	0.927	575°	539°	-3.39
New Berlin HS					
80-70C	B	0.942	?	378°	-8.13
80-70J	A	0.937	?	439°	-6.11
80-70K	C	0.945	?	341°	-9.53
80-70N	AA	0.939	?	417°	-6.82
80-70PP	C	0.951	?	<300°	-
80-70T	A	0.936	?	450°	-5.78
AVG(w/o PP)	(5)	0.940	?	404°	-7.22

Table 5. "Best spot" temperatures and sulfur fugacities for each sample as determined from pyrite-pyrrhotite electron microprobe analyses.

from the pyrrhotite composition is only 15°C below the peak metamorphic temperature estimated from the silicate and oxide phases. This is somewhat surprising considering the large degree of marcasite alteration observed surrounding the pyrrhotite grains. Perhaps some of the marcasite was formed by the migration of a sulfur-rich fluid through the rock, rather than pyrrhotite re-equilibration during retrograde conditions.

Mt. Finish Quarry. Of the sixteen samples collected from the Mt. Finish Quarry, only one (77-15Y) contained the assemblage pyrite + pyrrhotite. None of the remaining fifteen contained pyrrhotite; most contained pyrite, while some lacked sulfides altogether. The 450°C temperature determined from the pyrrhotite composition indicates that the pyrite and pyrrhotite re-equilibrated approximately 30°C below the estimated metamorphic peak. "Spot" B resulted in a temperature of 502°C. No significant marcasite alteration was observed.

Clough Brook. Two of the four samples analyzed contained pyrite + pyrrhotite. The two samples, 77-18M and 77-18X1 yielded vastly different temperatures - 354°C and 461°C respectively. The average temperature (408°C) for the two samples is meaningless because of the 110° difference between the two samples. Sample 77-18M must have re-equilibrated well below the peak metamorphic temperature. This is supported by the substantial marcasite rims observed around the pyrrhotite

grains. Sample 77-18X1 contains pentlandite and the pyrrhotite in equilibrium with the pyrite contained between 2.50 and 2.75 weight percent nickel. Assuming the nickel in the pyrrhotite is present as pentlandite, $(Fe_{3.4}Ni_{5.6})S_8$, rather than $NiFe_{-1}$ substitution, the temperature calculated from the "pure" pyrrhotite is 461°C, or 50°C below the assumed metamorphic peak. In general, the presence of substantial nickel in pyrrhotite would appear to make suspect any temperatures obtained from the pyrite-pyrrhotite geothermometer. Summarizing, pyrite-pyrrhotite geothermometry reveals no useful data regarding peak metamorphic temperatures encountered in the Clough Brook locality.

Wilder Dam. Pyrite is not present in either of the two samples analyzed from the Wilder Dam suite. Pyrite-pyrrhotite geothermometry could therefore not be applied to this suite.

Mt. Cube Quadrangle. Six of the eight Mt. Cube Quadrangle samples contain the assemblage pyrrhotite + pyrite. The average pyrite-pyrrhotite temperature for the suite is 482°C, or about 50°C below the assumed metamorphic peak. The average temperature derived from the highest temperature (lowest N_{FeS}) "spot" in each sample is 502°C, only 33°C below the peak of metamorphism. Four of the six samples are tightly clustered around the 502°C temperature (N_{FeS}=0.931) - 73-22E, 73-25A, 73-27C, and 77-58D. Data for sample 73-25B should be viewed somewhat skeptically, as it was the first sample to be probed

and inludes pyrrhotite analyses with totals ranging from 99.08 to 101.16. In addition, pyrrhotite grains in 73-25B have abundant marcasite alteration indicating retrograde re-equilibration. No similar reasons can be given for disregarding 73-31B, the other somewhat anomalous sample. The pyrrhotite totals appear reasonable and no marcasite alteration is observed. While 77-58D yields an average temperature of 512°C, it should be noted that the four individual "spots" in the sample yield widely varying temperatures - ranging from 390°C to 580°C. Pyrrhotite grains in sample 73-22E show substantial marcasite alteration, though the pyrite-pyrrhotite "spot" analyzed had minimal alteration and the resulting temperature was consistent with the rest of the suite. In summary, four of the six samples in the Mt. Cube Quadrangle suite yield a temperature of around 500°C, or 35°C below the estimated metamorphic peak.

North Grantham. Two samples analyzed from the North Grantham suite contained pyrite and pyrrhotite. The two samples, 80-28W and 80-28X, yielded very different temperatures - 492°C and 366°C respectively. Sample 80-28X has substantial marcasite rims around the pyrrhotite. In addition, the biotite in the sample is badly retrograded to chlorite. Both observations, in conjunction with the low pyrrhotite temperature, suggest that the observed mineral assemblage and compositions are not those of the peak of metamorphism. Sample 80-28W shows very strong pyrrhotite --→ marcasite alteration. In some grains the pyrrhotite has been completely

replaced by marcasite. Even "spot" C, which yields a 539°C temperature (~35° below the metamorphic peak), has approximately 50% marcasite alteration. So, in general, not much can be said for pyrite-pyrrhotite geothermometry in the North Grantham suite. Abundant retrograde sulfide textures are observed in the suite thereby making any pyrite-pyrrhotite temperature estimates suspect.

New Berlin High School. All six samples analyzed from the New Berlin High School rock cut contained euhedral pyrite in contact with pyrrhotite. The iron sulfides in 80-70PP have clearly re-equilibrated at very low temperatures, less than 250°C, and therefore equilibrated below the pyrrhotite hexagonal --→ monoclinic transition. Some of the pyrrhotite grains in 80-70PP are rimmed by chlorite and many are cut by chlorite needles. The average pyrrhotite temperature of the suite, excluding 80-70PP was determined to be 391°C. Both 80-70J and 80-70K contain more than 10% sulfides by volume. No positive explanation is offered for the different temperatures determined for the two similar samples, but microprobe totals for pyrrhotite in 80-70K are all greater than 100.25, suggesting that the standardization may have been poor. The average temperature for the suite, excluding both 80-70K and 80-70PP, is 404°C. The temperature of the peak of metamorphism for this suite is not known. Recent garnet-biotite temperatures for 80-70PP yield a temperature of 483±13°C (Peter Crowley, pers. comm.). This temperature must be held suspect as the pyrite-pyrrhotite temperature for

80-70PP indicates re-equilibration at very low temperatures. It was discussed earlier that this suite may have been subjected to polymetamorphism. It is conceivable that the second metamorphic event reset the pyrite-pyrrhotite geothermometer, but not the garnet-biotite geothermometer. The highest temperature obtained from a pyrite-pyrrhotite "spot" in the suite is 450°C for 80-70T ("spot" A), which is not inconsistent with the garnet-biotite temperature of 483°C for 80-70PP.

Sulfur Fugacity

The sulfur fugacity determined from pyrite-pyrrhotite equilibrium varies with temperature, as can be seen in Figure 16. Just as the geothermometry data is difficult to interpret, so is the sulfur fugacity data, only worse since no independent checks on the sulfur fugacity exist. Log $f(S_2)$ averages for each pyrite-pyrrhotite sample vary from -4.05 to -9.53, corresponding to a range in sulfur fugacity of five and a half orders of magnitude. The "best" (highest T) pyrite-pyrrhotite "spots" have an even larger variation in sulfur fugacity - greater than seven orders of magnitude. The 465°C to 570°C in estimated peak metamorphic temperatures should only result in a 2.70 range in log $f(S_2)$ if pyrite-pyrrhotite pairs reflected peak metamorphic conditions. No systematic variation in sulfur fugacity with increasing grade is observed. The Mt. Cube Quadrangle suite yielded the average sulfur fugacity (log $f(S_2)$ clustered around -4.32). This is

redundant since the same suite yielded the highest temperature, and both sulfur fugacity temperature are fixed by the assemblage pyrite + pyrrhotite (neglecting pressure).

Sulfur fugacity estimates for a single sample often vary widely. The 0.020 variation in N_{FeS} (pyrite-pyrrhotite pairs) observed in 77-58D corresponds to a range of over five orders of magnitude in sulfur fugacity. This strongly suggests that sulfur is not mobile in 77-58D, even on the centimeter scale. On the other hand, the pyrrhotite grains analyzed in 80-70N all had N_{FeS} values of 0.938 ± 0.001. Two of the three grains coexisted with pyrite, while the third pyrrhotite grain lacked pyrite and was altered partly to marcasite. The nearly identical composition for the three pyrrhotite grains suggests that sulfur may be mobile in 80-70N, at least on the centimeter scale.

Effects of Pressure

Toulmin and Barton (1964) calculated the effects of pressure on pyrite-pyrrhotite equilibrium from molar volume data, neglecting thermal expansion and compressibilty. They calculated the molar volume of pyrrhotite from the unit-cell-edge data of Haraldsen (1941) which was derived from experimentally synthesized pyrrhotites. Eliseev and Denisov's (1957) extensive investigation of natural pyrrhotites showed a wide scatter, and no apparent systematic variation, of molar volume with composition, hence their data was not used.

Toulmin and Barton calculated that:

$$\left(\frac{\partial N^{po}_{FeS}}{\partial P}\right)_{T,\Delta G=0} = 0.0018/kb \text{ at } 700°C, \text{ and } 0.0020/kb \text{ at } 325°C$$

The small value for $\partial N/\partial P$ sgrees well with the experimental results of Arnold (1962), who found no measurable effect on the composition of pyrrhotite in equilibrium with pyrite up to 2 kbars pressure. Toulmin and Barton also calculated the effect of pressure on the sulfur fugacity:

$$\left(\frac{\partial \log f_{S_2}}{\partial P}\right)_{T,\Delta G=0} = 0.28/kb \text{ at } 700°C, \text{ and } 0.50/kb \text{ at } 325°C$$

The effects of pressure on pyrite-pyrrhotite geothermometry in the Ammonoosuc Volcanics can be calculated assuming a confining pressure of ~5 kbars, a typical value cited for regional metamorphism. Taking the Mt. Cube Quadrangle as an example (N_{FeS} clustered at 0.931 --→ T = 500°C), the 5 kbar pressure would increase N_{FeS} to 0.941, thereby decreasing the calculated temperature to 391°C, a 110° decrease! Conversely log $f(S_2)$ would increase approximately two orders of magnitude.

It is not clear, however, whether the above pressure effects on the pyrite-pyrrhotite geothermometer are valid for natural rocks. Toulmin and Barton admitted to neglecting the more extensive data of Eliseev and Denisov (1957) on <u>natural</u> pyrrhotites, beacause of the lack of a systematic variation of

molar volume with composition. There is no reason to believe, therefore, that the calculated pressure effects are manifested in natural rocks.

Reflections on Pyrite-Pyrrhotite Geothermometry

It is apparent from the above discussion that pyrite-pyrrhotite equilibria can not be used to accurately determine peak metamorphic temperatures. All pyrite-pyrrhotite "spots" (with the single exception of 77-58D, "spot" C) appear to have re-equilibrated at temperatures lower than the metamorphic peak as determined from silicate and oxide data. Average pyrite-pyrrhotite temperatures vary from 15°C (Blood's Brook) to 130°C (North Grantham) below the peak metamorphic temperature. The effects of pressure on the geothermometer calculated by Toulmin and Barton (1964), if valid, only lower the pyrrhotite temperatures more. No clear systematic relationship between average pyrrhotite temperatures and actual peak temperatures is observed. Similarly, "best spot" temperatures do not appear to vary systematically with metamorphic grade. Retrograde alteration of pyrrhotite to marcasite usually results in a low pyrrhotite temperature, though the generalization does not hold for all samples.

The pyrite-pyrrhotite geothermometer may not be completely useless, however. The highest average temperature for any one sample in the suite does appear to vary systematically with metamorphic grade. The three low-grade suites have "best" sample average-temperatures of 450°C, 450°C,

and 461°C, while the two higher-grade suites have "best" samples of 512° and 492°C. The three low-grade suites average 30°C ("best" sample data) below the peak metamorphic temperature; the two high-grade suites average 50°C below the metamorphic peak. This suggests two conclusions - 1) that pyrite-pyrrhotite geothermometry may be valid for determining relative metamorphic grades if "best sample" data is used, and 2) the discrepancy between "best sample" pyrite-pyrrhotite and peak metamorphic temperatures increases with increasing metamorphic grade. In summary, pyrite-pyrrhotite geothermometry may be useful in determining relative differences in metamorphic grade, though absolute temperatures can not be determined with the geothermometer. Also, and perhaps most importantly, the difference between the pyrrhotite temperature and the peak metamorphic temperature may reflect differences in the cooling rate.

VII. THE NATURE OF THE PYRITE --→ PYRRHOTITE REACTION

Possible Reactions

One of the goals of this research was to determine, if possible, the reaction(s) responsible for the conversion of pyrite to pyrrhotite. There are three possible types of reactions; 1) iron depletion, 2) iron metasomatism, and 3) desulfurization. These reactions can be represented schematically as:

(1) $\underset{\text{pyrite}}{FeS_2} + \underset{\text{silicate or oxide}}{FeO} = \underset{\text{pyrrhotite}}{2FeS} + \underset{\text{fluid}}{\frac{1}{2}O_2}$

(2) $\underset{\text{pyrite}}{FeS_2} + \underbrace{FeCl_2 + H_2O}_{\text{fluid}} = \underset{\text{pyrrhotite}}{2FeS} + \underbrace{4HCl + \frac{1}{2}O_2}_{\text{fluid}}$

(3) $\underset{\text{pyrite}}{FeS_2} + \underset{\text{fluid}}{H_2O} = \underset{\text{pyrrhotite}}{FeS} + \underbrace{H_2S + \frac{1}{2}O_2}_{\text{fluid}}$

Evidence supporting reactions (1) and (3) has been presented in the literature in studies on various different rock types, whereas reaction (2) - iron metasomatism - has never been documented. Several authors have argued that iron depletion of surrounding phases (i.e. reaction (1)) is required for the conversion of pyrite to pyrrhotite in metapelites (Thompson, 1972; Robinson et al., 1976). Other researchers have presented evidence showing that sulfur is mobilized during the metamorphism of certain ore deposits

(Fullagar et al., 1967; Vokes, 1971). Ferry (1981) has demonstrated that pyrite reacts to form pyrrhotite via desulfurization (i.e. reaction (3)) in graphitic schists from Maine. Ferry went on to conclude that the reaction is driven by the flow of fluid through the rock, which removes the sulfur produced by the reaction. Evidence from my study of sulfides in the metamorphosed Ammonoosuc Volcanics support desulfurization as the mechanism for the pyrite --→ pyrrhotite transition, as will be documented below.

Problems Encountered

The nature of the Ammonoosuc Volcanics, and metavolcanics in general, preclude the use of bulk chemistry data as an aid in determining the pyrite --→ pyrrhotite reaction. Such data was used by Ferry (1981) in metapelites to help demonstrate that pyrite was converted to pyrrhotite at constant whole rock Fe-contents. Ferry was able to follow a single rock unit (with the same bulk composition) through a series of metamorphic isograds and could therefore ignore the effects of bulk composition differences on the reaction. In contrast, the Ammonoosuc Volcanics are chemically inhomogeneous, even on the scale of a single outcrop. Like most submarine volcanic sequences, the Ammonoosucs consist of a varying mixture of volcanics and sediments. The volcanics themselves have a variable composition and in places may have suffered hydrothermal alteration on the sea-floor. Therefore, it is very difficult to trace an isochemical unit through a

sequence of isograds in metavolcanics such as the Ammonoosuc Volcanics.

The poor outcrop exposure in New Hampshire and Vermont also hindered my study. Reactions (1) and (2) both result in two moles of pyrrhotite being produced for every one mole of pyrite consumed, while reaction (3) only produces one mole of pyrrhotite. Thus, if an isochemical layer could be identified and followed through the broad pyrite-pyrrhotite "isograd", it is possible that the sulfide modal abundance data could constrain the reaction-type. Unfortunately, the poor outcrop exposure, in addition to the inhomogeneous composition of the rocks, have made it impossible to identify and follow an isochemical layer in the Ammonoosuc Volcanics.

For the reasons cited above, the nature of the pyrite --→ pyrrhotite reaction in the Ammonoosuc Volcanics is difficult to define, more so than in metapelites.

Controlling Factors of the Pyrite --→ Pyrrhotite Reaction

As was mentioned earlier in several chapters, the coexistence of pyrite + pyrrhotite over a wide range in metamorphic grade strongly suggests that temperature is not the dominant controlling factor of the pyrite --→ pyrrhotite reaction. Bulk chemical analyses are not available on any of the samples, but no clear differences in the mineralogy of pyrite + pyrrhotite samples is observed. If it assumed that the bulk composition of the rock is not the controlling factor, then in order to be viable, each of the three possible

reactions must have a rate controlling step that is not a strong function of temperature.

Reaction (1), iron-depletion, is probably controlled by the rates of the Fe-bearing phase breakdown reaction and grain boundary diffusion. The extent of the pyrite --→ pyrrhotite reaction observed would be a function of the amount of iron released by other minerals. Reactions (2) and (3) are controlled by the rate of fluid flow through the rock; reactions (2) and (3) require initially Fe-rich and S-poor fluids, respectively. The rates of reactions (2) and (3) would depend on the fluid:rock ratio, the fluid pressure gradient, temperature, and the initial composition of the fluid.

Iron-Depletion

Reactions of type (1) require the removal of iron from another phase in order to produce pyrrhotite from pyrite. Hornblende and biotite are the two most abundant Fe-bearing phases in the Ammonoosuc Volcanics. Biotite within an ore deposit is commonly reported to be less Fe-rich than biotite in the wall rock (e.g. Fullagar et al., 1967). Iron cannot be removed from biotite without breaking down the biotite structure (i.e. through a reaction such as annite + O_2 --→ kspar + magnetite + H_2O). Therefore, if biotite is the source of iron for the pyrite --→ pyrrhotite transition, one would expect to see potassium feldspar. No K-spar is observed in any of the 27 samples, so unless potassium has been removed

from the system, in all eight localities, biotite can not be the source of iron. FeO could be removed from hornblende, via a reaction such as Fe-pargasite --→ plagioclase + magnetite + qtz + H_2O. Plagioclase is present in nearly every sample, and alumino-silicate is consumed by the reaction and therefore may no longer be present if this reaction has occurred. Thus, it is possible, though unlikely, that hornblende provided FeO for the pyrite --→ pyrrhotite reaction. No reaction texture suggesting the breakdown of hornblende was observed in any sample.

In a brief attempt to check for iron-depletion of silicate phases in several samples were analyzed with the electron microprobe for Fe-zoning near pyrrhotite grains. While cummingtonite showed no significant zoning, Fe/Fe+Mg ratios for biotite and hornblende <u>increased</u> slightly as the pyrrhotite grain was approached (see Appendix V). The reasons for this "reverse" zoning are not known. Many more samples need to be analyzed before any definite conclusions can be drawn.

Ilmenite commonly contains up to six weight percent ferric iron. FeO could be produced from ilmenite by reducing some of the ferric iron, thereby increasing the Ti/Fe ratio of the ilmenite. A microprobe survey of ilmenite grains in seven samples revealed five samples in which grains close to or touching pyrrhotites were an average of 0.84 weight percent <u>lower</u> in Fe, than ilmenite grains distant from pyrrhotite. Individual ilmenite grains were not zoned. The modal amount

of ilmenite in any of the samples is rarely greater than 1 %. A quick calculation, assuming one-half of the ilmenite is depleted in iron by 2 wt % (the maximum depletion observed), reveals that the amount of iron released could not account for more than 2.5 % of the pyrite --→ pyrrhotite reaction (assuming 1.0 volume % initial pyrite). Thus, iron-depletion of ilmenite can not be responsible for significant amounts of pyrrhotite formation.

Iron Metasomatism

Pyrite could be converted into pyrrhotite by the addition of Fe to the system - reaction (2). No cases of regional iron metasomatism have been reported in the literature. The fluid transport of significant amounts of iron is apparently confined to hydrothermal veins and surficial weathering. It is therefore highly improbable that Fe-rich fluids were responsible for the widespread pyrite --→ pyrrhotite transition observed in the Ammonoosuc Volcanics.

No mineralogical or textural observations (such as extensive Fe-Mg zoning in the silicates, or abundant magnetite) suggest that significant iron metasomatism had ever taken place in the Ammonoosuc Volcanics. Moreover, the modal amount of magnetite observed in a sample does not appear to have any relation to the extent of the pyrite --→ pyrrhotite reaction.

Desulfurization

The third possible pyrite --→ pyrrhotite reaction requires the removal of sulfur from the system - reaction (3). Desulfurization has been well-documented by Ferry (1981) to be responsible for the pyrite --→ pyrrhotite transition observed in graphitic schists from Maine. Leaving out his more elaborate arguments, iron-depletion is easily ruled out in his area because of the lack of sufficient amounts of iron in the non-sulfide phases. Unfortunately, the same can not be said for the Ammonoosuc Volcanics which contain abundant Fe-Mg silicates.

The positive correlation of "marcasite alteration of pyrrhotite" with the "presence of pyrite" in the 27 samples strongly suggests that pyrite is transformed to pyrrhotite by releasing sulfur into the fluid phase. Of the 15 samples in which pyrrhotite is altering to marcasite, 13 also contain pyrite. On the other hand, of the 12 samples lacking marcasite alteration, only 5 contain pyrite. Marcasite alteration of pyrrhotite appears to occur exclusively as rims on pyrrhotite grains and along cracks. This is very good evidence that the pyrrhotite --→ marcasite reaction involves introduction of sulfur from a fluid phase. So, why is this alteration texture significantly more common in samples containing pyrite?

The following sequence of events represents a possible explanation for the marcasite correlation: Sulfur is released into the fluid phase as pyrite is transformed into pyrrhotite

via reaction (3). The amount of sulfur in the fluid surrounding the sulfide grains will quickly buffer the reaction progress, assuming that reaction kinetics are rapid. So, in order for the reaction to proceed, sulfur must be continuously removed from the system by the flushing of sulfur-poor fluids through the rocks (a similar scenario was presented by Ferry, 1981). In rocks where fluid flow was sufficiently high, the reaction went to completion (i.e. no remaining pyrite). In rocks where the fluid flow was limited, the reaction progressed to a degree comensurate with the fluid:rock ratio. The presence of pyrite in many samples indicates that the pyrite --→ pyrrhotite reaction did not continue to completion. The reaction presumably was halted when the temperature dropped or the flow of fluid through the rock came to a stop. In either case, substantial amounts of sulfur will be left in the surrounding fluid phase in a rock that contains pyrite and pyrrhotite. This sulfur is then available to react with the pyrrhotite to form marcasite along grain boundaries and cracks as the rock cools. Why metastable marcasite is precipitated rather than pyrite is not clear; it is suggested that the answer may lie in the nucleation kinetics of the two FeS_2 phases. For what ever reason, marcasite is the most common alteration of pyrrhotite according to Ramdohr (1969).

If a decrease in temperature was responsible for the pyrite --→ pyrrhotite reaction coming to a halt, then FeS_2 would quickly become the stable iron-sulfide phase, as

conditions passed into the FeS_2 stability field (see Fig. 16); thus sulfur in the fluid will react to form marcasite. Similarly, if the pyrite --→ pyrrhotite reaction was stopped because fluid flow through the rock ceased, the sulfur will remain in the fluid phase until the temperature decreases into the FeS_2 stability field.

In principle, it would be possible to calculate the amount of fluid necessary to to account for a given amount of reaction progress, if the composition of the fluid flushing through the rock were known. However, no assemblages enabling calculation of fluid composition have been identified.

The lack of marcasite in most samples containing pyrrhotite and no pyrite can be explained by the absence of significant sulfur in the fluid phase when the rock cooled. In this case, all the sulfur was flushed out earlier by the fluids, as is indicated by the completed pyrite --→ pyrrhotite reaction. The presence of marcasite in some pyrrhotite-only samples, can be explained simply by a sulfur-rich fluid passing through the rock when the temperature was in the FeS_2 stability field. The sulfur could possibly be derived from a nearby pyrite --→ pyrrhotite reaction. Large amounts of sulfur-rich fluids passing through the rock are proposed for samples with substantial marcasite alteration.

In Chapter III, it was noted that the composition of pyrrhotite grains in pyrite-bearing samples varied systematically according to whether or not the pyrrhotite was in physical contact with the pyrite. The composition of

pyrrhotites in contact with pyrite are significantly more Fe-rich (ΔN_{FeS} = +0.003) than the composition of isolated pyrrhotites in the same sample. This observation can be explained by the following sequence of events consistent a the desulfurization pyrite --→ pyrrhotite reaction mechanism. Figure 17 shows an enlarged portion of the log $f(S_2)$ vs. T diagram depicted in Figure 16. At T_1, the peak temperature of metamorphism, a "spot" containing pyrite + pyrrhotite in equilibrium with a sulfur-rich fluid will be fixed at point A. Point B represents a pyrrhotite grain in the same sample, but located in a pyrite-absent "spot". If the "spot" B pyrrhotite is in equilibrium with the same fluid as "spot" A, then both points will be coincident at point A. If not, then point B will most likely plot slightly beneath point A (e.g. this would happen if the flow of fluids through the rock ceased).

As the rock starts to cool, "spot" B will proceed towards B' along a sulfur fugacity isopleth. Marcasite will probably not form exactly at the pyrite-pyrrhotite univariant curve because of nucleation problems. "Spot" A is constrained to follow the pyrite-pyrrhotite equilibrium curve as the rock cools, and will therefore move towards point A'. Thus, at some $T_2 < T_1$, when the iron sulfides stop equilibrating, the pyrrhotite in "spot" A will be more Fe-rich than the "spot" B pyrrhotite. Summarizing, a pyrite-pyrrhotite pair is restricted to cooling along its univariant equilibrium curve, while an isolated pyrrhotite grain will most likely cool at a constant sulfur fugacity.

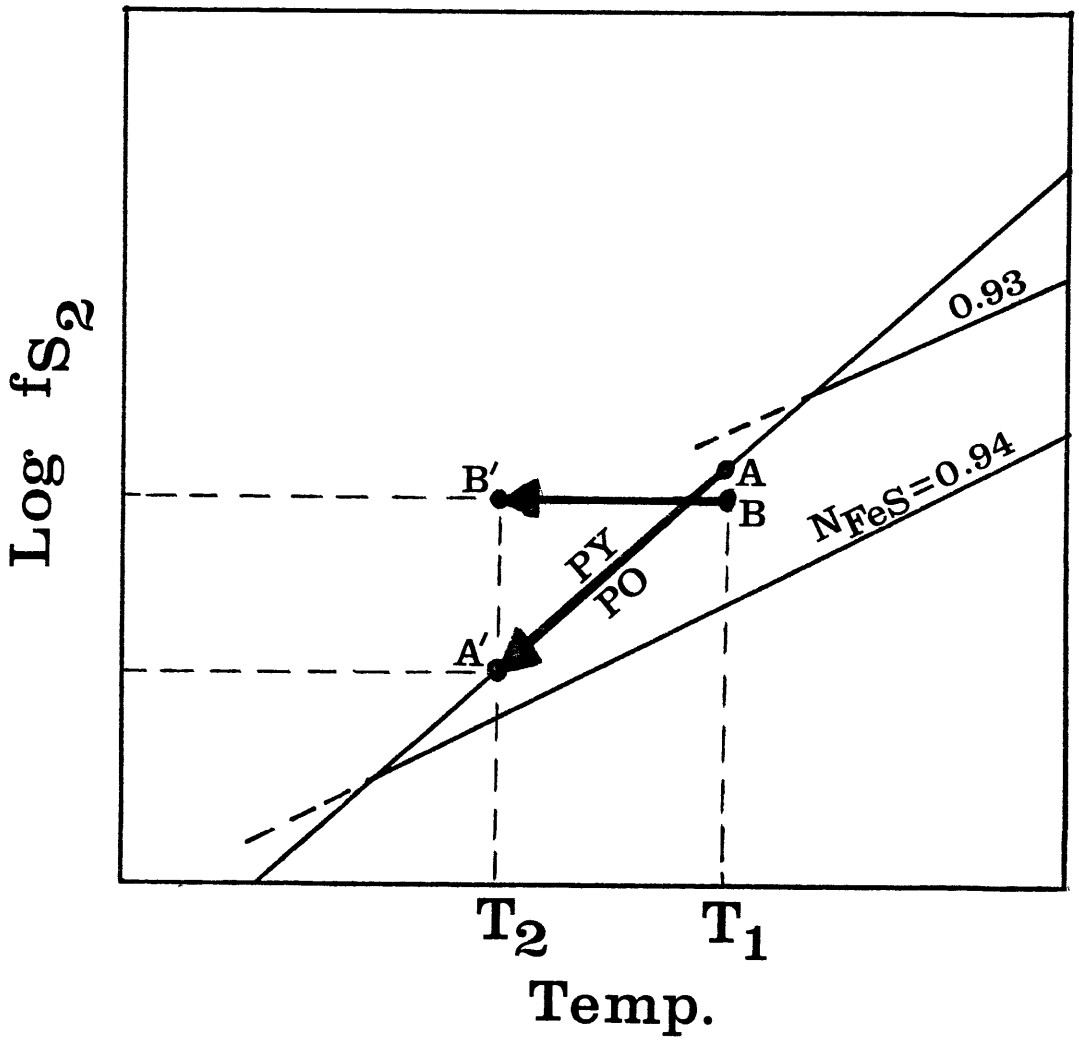

Figure 17. Enlarged portion of Figure 16, path A → A' represents cooling of pyrite and pyrrhotite in equilibrium. Path B → B' represents the cooling path followed by an independent pyrrhotite grain.

If the above model is correct, then it implies that isolated pyrrhotite grains in a pyrite-bearing sample will more accurately reflect peak metamorphic temperatures. No well-defined decrease in N_{FeS} is observed with increasing metamorphic grade for "spot" B-type pyrrhotites (see Appendix II). Rather, the pyrrhotite composition apppears to be fairly constant, $N_{FeS} \sim 0.931$, within the accuracy of the data. Not unsurprisingly, isolated pyrrhotites from the New Berlin High School suite have widely fluctuating compositions.

Neither pyrite-pyrrhotite reactions (1) or (2) can account for the marcasite correlation. The iron depletion reaction does not affect the fluid phase and thus cannot explain the pyrrhotite --→ marcasite alteration. If the pyrite --→ pyrrhotite reaction was caused by iron-metasomatism, then the reaction would stop (i.e. pyrite and pyrrhotite would be present) if the temperature dropped or the fluid flow ceased. In this scenario, a decrease in temperature would result in Fe-rich fluids flowing past pyrite+pyrrhotite in the FeS_2 stability field; marcasite would <u>not</u> be produced under these conditions. If the fluid flow had ceased, then any remaining Fe in the fluid should react with the pyrite to form pyrrhotite, and the reaction would end; again, there is no reason that marcasite should form in this environment.

I therefore conclude that the positive correlation between marcasite alteration of pyrrhotite and the presence of pyrite (incomplete pyrite --→ pyrrhotite reaction) in a rock

can only be explained by one of the three possible pyrite --→ pyrrhotite reactions - desulfurization (reaction (3)). Moreover, desulfurization is the only mechanism that adequately explains the sequence pyrite --→ pyrrhotite --→ marcasite.

Thus, the same desulfurization reaction mechanism proposed by Ferry (1981) for metapelites from Maine, is believed to operate in the more Fe-rich, metavolcanics from New Hampshire and Vermont.

VIII. CONCLUSIONS AND IMPLICATIONS

Iron-sulfide textures contain important information about the behavior of sulfur in volcanic rocks during metamorphism. Three distinct sulfide textures are observed in the regionally metamorphosed Ammonoosuc Volcanics. The three textures are interpreted as (1) a prograde pyrite --→ pyrrhotite reaction, (2) a retrograde pyrrhotite --→ marcasite reaction, and (3) a marcasite --→ secondary "pyrite" reaction that may be evidence of a second metamorphic event.

Modal analyses of 150 samples from the Ammonoosuc Volcanics document the conversion of pyrite to pyrrhotite with increasing metamorphic grade. Pyrite and pyrrhotite coexist over a wide range in metamorphic grades, suggesting that temperature is not the only factor controlling the pyrite --→ pyrrhotite reaction. Microprobe analyses of pyrrhotite grains indicate that pyrite-pyrrhotite geothermometry may be valid for determining relative metamorphic grades if "best sample" data is used. Temperatures calculated with the geothermometer are always lower than the estimated peak temperature of metamorphism. The differences between the calculated and peak temperatures may reflect differences in cooling rates.

A strong positive correlation is observed between marcasite alteration of pyrrhotite and the presence of pyrite in the same sample. This correlation strongly suggests that desulfurization is the dominant pyrite --→ pyrrhotite reaction, despite the abundance of iron in coexisting

silicates and oxides. The flow of fluids through the rock serves as the driving mechanism for the desulfurization reaction, similar to the mechanism proposed by Ferry (1981) for metapelites from Maine. The extent of the pyrite --→ pyrrhotite reaction is dependent on the fluid:rock ratio, the fluid pressure gradient, temperature, and the initial composition of the fluid.

This study has shown that significant transport of sulfur does occur during metamorphism. The next logical step is to try and follow the sulfur's course through the rock, perhaps using sulfur isotopes. It seems reasonable to expect the sulfur to precipitate from the fluid while it is still within the rock. The ability to locate these precipitation sites may lead to the discovery of new ore deposits.

REFERENCES

Alcock, C.B. and Richardson, F.G. (1951) Thermodynamics of ferrous sulphide. Nature, London, 168, 661-662.

Andrews, Anthony J. (1979) On the effect of low temperature sea-water basalt interaction on the distribution of sulfur in oceanic crust, layer 2. EOS(abstr.), 60, 973.

Arnold, R.G. (1962) Equilibrium relations between pyrrhotite and pyrite from 325° to 743°C. Econ. Geol., 57, 72-90.

Bachinski, D. J. (1976) Metamorphism of eupriferous iron sulfide deposits, Notre Dame Bay, Newfoundland. Econ. Geol., 71, 443-452.

Banno, S. and Kanehira, K. (1961) Sulfide and oxide minerals in schists of the Sanbagawa and Central Abukuma metamorphic terranes. Japan Jour. Geol. Geogr., 32, 331-348.

Barton, P.B., Bethke, P.M., and Toulmin, P. (1963) Equilibrium in ore deposits. Min. Soc. Amer., Spec. Paper 1, 171-185.

_____ and Skinner, B.J. (1967) in Geochemistry of Hydrothermal Ore Deposits (H.L. Barnes ed.). Holt, Rinehart, and Winston: New York, 670p.

Bezmen, N.I. and Smolyarova, T.A. (1977) Enthalpy of formation of monoclinic pyrrhotite and its stability in the system Fe-S. Int. Geol. Rev., 19, 761-765.

_____ and Tikhomirova, V.I. (1975) The effect of temperature on distribution of cobalt and nickel between iron sulfides and solutions of different composition. Geochem. Int., 12, 59-65.

_____, _____, and Kosogova, V.P. (1975) Pyrite-pyrrhotite geothermometer: partition of Ni and Co. Geochem. Int., 12, 45-59.

Berry, W.B.N. (1962) On the Magog, Quebec, graptolites. Amer. Jour. Sci., 260, 142-148.

Billings, M.P. (1956) The Geology of New Hampshire, Part II - Bedrock Geology. N.H. Plan and Development Comm., 203p.

Boucot A.J. (1961) Stratigraphy of the Moose River Synclinorium, Maine. U.S.G.S. Bull., 1111-E, 118p.

REFERENCES (cont.)

Butler, P. (1969) Mineral compositions and equiliria in the metamorphosed iron formation of the Gagnon region, Quebec, Canada. Jour. Petrol, 10, 56-101.

Cady W.M. (1960) Stratigraphic and geotectonic relationships in northern Vermont and southern Quebec, GSA Bull., 71, 531-560.

Carpenter, R.H. (1974) Pyrrhotite isograd in southeastern Tennesssee and southwestern North Carolina. GSA Bull., 85, 451-456.

_____ and Desborough, G.A. (1964) Range in solid solution and structure of naturally occurring troilite and pyrrhotite. Amer. Min., 49, 1350-1365.

Clark, R. and Naldrett, A.J.. (1972) The distribution of Fe and Ni between synthetic oliovine and sulfide at 900°C. Econ. Geol., 67, 939-952.

Deb, M. (1980) Genesis and metamorphism of two stratiform massive sulfide deposits at Ambaji and Deri in the Precambrian of Western India. Econ. Geo., 75, 572-591.

Desborough, G.A. and Carpenter, R.H. (1965) Phase relations of pyrrhotite. Econ. Geol., 60, 1431-1450.

Doll, G.G., Cady, W.M., Thompson, J.B.Jr., and Billings, M.P. (1961) Centennial Geologic Map of Vermont: Verm. Geol. Survey, Montpelier, Vt. Scale 1:250,000.

Downes, W.F. and Deines, P. (1978) Experimental calibration of the quartz-magnetite oxygen isotope geothermometer (abstr) GSA Abstracts w/ programs, 10, 392.

Eremin, N.I. (1978) Variations in the composition of ore-forming sulfides and the conditions of formation of pyritic ore bodies. Mosc. Univ. Geol. Bull., 33, 43-49.

Ferry, J.M. (1981) Petrology of graphitic sulfide-rich schists from south-central Maine: an example of desulfidation during prograde regional metamorphism. Amer. Min., upcoming issue.

_____ and Spear, F.S. (1978) Experimental calibration of the partitioning of Fe and Mg between garnet and biotit biotite. Contrib. Min. Petrol., 66, 113-117.

Froese, E. and Gunter, A.E. (1976) A note on the pyrrhotite-sulfur vapor equilibrium. Econ. Geo., 71, 1589-1594.

REFERENCES (cont.)

Froese, E. (1971) The graphical representation of sulfide-silicate equilibria. Econ. Geol., 66, 335-341

Fullagar, P.D., Brown, H.S. and Hagner, A.F. (1967) Geochemistry of wall rock alteration and the role of sulferization in the formation of the ore knob sulfide deposit. Econ. Geol., 62, 798-825.

Guidotti, C.V. (1970) The mineralogy and petrology of the transition from the lower to upper sillimanite zone in the Oquossoc Area, Maine. Jour. of Petrology, 11, 277-336.

_____, Cheney, J.T., and Henry, D.J. (1977) Sulfide-silicate phase relations in metapelites of northwestern Maine. Amer. Geophy. Union/Trans. (abstr.), 58, 524.

Harwood D.S. (1966) Geology of the Cupsitic Quadrangle, Maine. USGS open file report 850, 259p.

_____ and Berry, W.B.N. (1967) Fossiliferous lower Paleozoic rocks in the Cupsuptic quadrangle, west-central Maine. U.S.G.S. Prof. Paper 575-D, D16-D23.

Hekinian, R., Feurier, M., Bischoff, J.L., Picot, P., Shanks, W.C. (1980) Sulfide Deposits from the East Pacific Rise near 21°N. Science, 207, 1433-1444.

Hutcheon, I. (1978) Calculation of metamorphic pressure using the sphalerite-pyrrhotite-pyrite equilibrium. Am. Min. 63, No. 1-2, 87-95.

Kanehira, K., Banno, S., Nishida, K. (1964) Sulfide and oxide minerals in some metamorphic terrains in Japan. Japanese Jour. Geology Geography, 35, 175-191.

Kinkel, A.R., Jr. (1967) The ore knob copper deposit, North Carolina, and other massive sulfide deposits of the Appalachians. USGS Prof. Paper 558, 1-58.

Kuebler, L. (1978) The influence of stress on the formation of monoclinic pyrrhotite. Acta Univ. Ups., No 451, 11p.

REFERENCES (cont.)

Kullerud, G. and Yoder, H.S. (1959) Pyrite stability relations in the Fe-S system. Econ. Geo., 54, 533-572.

_____ and _____ (1963) Sulfide-silicate relations. Carnegie Inst. Wash. Year Book, 62, 226-230.

_____ and _____ (1964) Sulfide-silicate relations. Carnegie Inst. Wash. Year Book 63, 218-222.

Mallio, W.J. and Gheith, M. A. (1972) Textural and chemical evidence bearing on sulfide-silicate reactions in medisediments. Min. Deposita, 7, 13-17.

McDonald, J.A. (1967) Metamorphism and its effects on sulphide assemblages. Min. Deposita, 2, 200-220.

Morimoto, N., Nakazawa, H., Nishiguchi, K., and Tokonami, M. (1970) Pyrrhotites: stoichiometric compounds with composition $Fe_{n-1}S_n(n\geq 8)$. Science, 168, 964-966.

Naldrett, A.J. (1966) The role of sulfurization in the genesis of iron-nickel sulfide deposits of the Porcupine District, Ontario. Can. Min. Metall. Bull., 69, 147-155.

_____ and Brown, G.M. (1968) Reaction between pyrrhotite and enstatite-ferrasilite solid solutions. Carnegie Inst. Wash. Yearbook, 66, 427-429.

Popp, R.K., Gilbert, M.C. and Craig, J.R. (1977) Stability of Fe-Mg amphiboles with respect to sulfur fugacity. Amer. Min., 62, 13-30.

Robinson, P. and Tracy, R.J. (1977) Sulfide-silicate-oxide equilibria in sillimanite-K-feldspar grade pelitic schists, Central Massachusetts. Amer. Geophy. Union/ Trans. (abstr.), 58, 524.

Sarkar, S.C., Bhattacharyya, P.K., Mukherjee, A.D. (1980) Evolution of the sulfide ores of Saladipura, Rajasthan, India. Econ. Geol., 75, 1152-1167.

Sillitoe, R.H. (1973) Environments of formation of vocanogenic massive sulfide deposits. Econ. Geol., 68, 1321-1336.

Steger, J.F. and Desjardins, L.E. (1978) Oxidation of sulfide minerals: 4, pyrite, chalcopyrite, and pyrrhotite. Chem. Geol., 23, 225-237.

REFERENCES (cont.)

Starton, R.L. (1964) Mineral interfaces in stratiform ores. Inst. Min. Metall., 74, 45-79.

Thompson, J.B. Jr. (1972) Oxides and sulfides in regional metamorphism of pelitic schists. 24th IGC, Section 10.

Thompson, J.B. Jr., Robinson, P., Clifford, T.N., and Newell, N.J. Jr., Nappes and gneiss domes in west-central New England. in: Studies on Appalachian Geology Northern and Maritime (ed. Zen, White, Hadley, Thompson) Interscience Publ.: New York, 475 pp.

Toulmin, P. and Barton P.B. (1964) A thermodynamic study of pyrite and pyrrhotite. Geochim. Cosmochim. Acta, 28, 641-671.

Upadhyay, H.D. and Smitheringale, W.G. (1972) Geology of the Gullbridge copper deposit, Newfoundland: volcanogenic sulfides in cordierite-anthophyllite rocks. Can. J. Earth Sci., 9, 1060-1073.

Vokes, F.M. (1968) Regional metamorphism of the Paleozoic geosynclinal sulphide ore deposits of Norway. Inst. of Mining and Metallurgy, Trans., 77, B53-59.

_____ (1969) A review of the metamorphism of sulphide deposits. Earth-Sci. Rev., 5, 99-143.

_____ (1971) Some aspects of the regional metamorphic remobilization of pre-existing sulfide deposits. Min. Deposita, 6, 122-129.

Williams, D., Stanton, R.L. and Ramband F. (1977) The Planes-San Antonio pyritic deposit of Rio Tinto, Spain: its nature, environment, and genesis. in: Volcanic Processes in Ore Genesis, Chameleon Press Ltd.: London, 152.

Williamson, T.C. and Myer, G.H. (1969) A pyrrhotite-pyrite isograd in the Waterville area, Maine. GSA Abs, w/Programs for 1969, Pt. 7, (Ann. Mtg.), 237.

Zavaritsky, A.N. (1950) Metasomatism and metamorphism in the pyrite deposits of the Urals. Int. Geol. Congress 18th session, London, 1948, Report Part 3, 102-117.

APPENDIX I - SULFIDE STANDARDS

ELEMENT	NAME	Fe	S	Cu	Ni	Co	Zn
Co,Fe,S	CoFeS	60.74	38.73	-	-	0.53	-
Cu	Cpy	30.43	34.94	34.62	-	-	-
Ni	NiFeS	55.59	38.60	-	5.79	-	-
Zn	ZnO	-	-	-	-	-	81.33

Working Standards

ELEMENT	NAME	Fe	S
Fe,S	Synthetic Pyrrhotite	61.00	39.00
Fe,S	Synthetic Troilite	63.527	36.473

APPENDIX II - MICROPROBE ANALYSES - PYRRHOTITE

SAMPLE	"SPOT"	# OF ANAL.	COEXISTING SULFIDES	N_{FeS}	T(°C)	LOG f(S2)
			BLOODS BROOK			
77-23D	A	9	Py,Marc	0.936	450°	-5.78
	B	6	Py,Marc	0.936		
	C	9	Cpy,Marc	0.933		
	AVG.	(3)		0.935		
	AVG(PY-PO)	(2)		0.936	450°	-5.78
			MT. FINISH QUARRY			
77-15Y	B	4	Py	0.931	502°	-4.32
	C	9	Py	0.936	450°	-5.78
	D	3	Cpy	0.932		
	E	4	Py,Cpy	0.940	404°	-7.22
	AVG.	(4)		0.935		
	AVG(PY-PO)	(3)		0.936	450°	-5.78
			CLOUGH BROOK			
77-18M	A	6	Py,Cpy	0.944	354°	-9.00
77-18O	A	12	Cpy	0.934		
	AA	14	-	0.934		
	B	13	Cpy	0.933		
	C	12	Cpy	0.933		
	AVG.	(3)		0.933		
77-18P	A	4	Cpy	0.951		
	C	4	-	0.939		
	D	3	-	0.946		
	AVG.	(3)		0.945		
77-18X1	A	3	Py,Cpy	0.935*	461°	-5.47
	B	4	Py,Pent,Cpy	0.924	**	**

* - N_{FeS} value was calculated assuming all Ni in pyrrhotite was present as pentlandite impurity (see text).

** - The N_{FeS} value of 0.924 is invalid because of widely fluctuating totals, hence temperature and sulfur fugacity values are not reported.

APPENDIX II - MICROPROBE ANALYSES - PYRRHOTITE (cont.)

SAMPLE	"SPOT"	# OF ANAL.	COEXISTING SULFIDES	N_{FeS}	T(°C)	LOG $f(S_2)$
			WILDER DAM			
77-20G	A	5	Co-S	0.938		
	B	3	Cpy	0.941		
	BB	3	Cpy	0.954		
	F	3	-	0.948		
	AVG.	(3)		0.945		
77-20N	A	5	-	0.930		
	B	3	Cpy	0.934		
	D*	1	-	0.943		
	E*	1	Cpy	0.913		
	AVG.	(2)		0.932		
			MT. CUBE QUADRANGLE			
73-22E	A	10	Marc	0.934		
	B	9	Py	0.932	492°	-4.59
	C	9	Marc	0.933		
	C-BAND**	6	Marc	0.943		
	D	10	Cpy,Marc	0.931		
	AVG.	(4)		0.9325		
73-25A	A	13	Py	0.932	492°	-4.59
	B	13	Py	0.931	502°	-4.32
	AVG.	(2)		0.9315	497°	-4.46
73-25B	A	5	Py,Cpy	0.938	428°	-6.46
73-26A	A	5	-	0.930		
	F	2	Cpy	0.936		
	AVG.	(2)		0.933		

* - Excluded from the average because only one analysis was obtained.

** - The anomalously Fe-rich band was excluded from the average.

APPENDIX II - MICROPROBE ANALYSES - PYRRHOTITE (cont.)

SAMPLE	"SPOT"	# OF ANAL.	COEXISTING SULFIDES	N_{FeS}	T(°C)	LOG f(S2)
			MT. CUBE QUADRANGLE (cont.)			
73-27C	C	4	Py,Cpy	0.931	502°	-4.32
73-30M	A	3	Asp	0.943		
	C*	1	Asp	0.947		
	F	4	Asp	0.947		
	AVG.	(2)		0.945		
73-31B	A	6	Py,Cpy	0.937	439°	-6.11
	B	5	Py,Cpy	0.933	482°	-4.86
	C	3	-	0.929		
	D	3	-	0.929		
	AVG.	(4)		0.932		
	AVG(PY-PO)	(2)		0.935	461°	-5.47
77-58D	A	7	Py,Cpy	0.932	492°	-4.59
	B	2	Py,Cpy,Marc	0.924	566°	-2.76
	C	6	Py,Cpy	0.922	583°	-2.36
	E	4	Py,Cpy	0.942	378°	-8.13
	AVG.	(4)		0.930	512°	-4.05
			NORTH GRANTHAM			
80-28O	A	15	-	0.932		
	AA	7	Cpy	0.934		
	B	5	-	0.937		
	C	7	-	0.934		
	D	8	-	0.932		
	AVG.	(4)		0.934		
80-28T	A	7	-	0.932		
	AA	8	-	0.929		
	AAA	4	Cpy	0.930		
	B	7	-	0.928		
	C	7	-	0.929		
	AVG.	(3)		0.929		

* - Excluded from average because only one analysis was obtained.

APPENDIX II - MICROPROBE ANALYSES - PYRRHOTITE (cont.)

SAMPLE	"SPOT"	# OF ANAL.	COEXISTING SULFIDES	N_{FeS}	T(°C)	LOG f(S_2)
			NORTH GRANTHAM (cont.)			
80-28U	A	7	-	0.933		
	AA	9	Cpy	0.933		
	B	8	-	0.932		
	BB	9	Cpy	0.932		
	C	4	Cpy	0.930		
	D	7	-	0.933		
	AVG.	(4)		0.932		
80-28W	A	5	Py,Cpy	0.941	391°	-7.68
	AA	11	Marc	0.932		
	C	8	Py	0.927	539°	-3.39
	D	10	-	0.934		
	F	4	-	0.932		
	AVG.	(5)		0.933		
	AVG.(PY-PO)	(2)		0.934	472°	-5.16
80-28X	A	14	Marc	0.942		
	C	6	Marc	0.943		
	AVG.	(2)		0.9425		
			NEW BERLIN HIGH SCHOOL			
80-70C	B	10	Py,Cpy	0.942	378°	-8.13
	C	8	Marc	0.940		
	AVG.	(2)		0.941		
80-70J	A	13	Py,Cpy	0.937	439°	-6.11
	B	21	Py,Cpy	0.941	391°	-7.68
	D	11	????	0.940		
	AVG.	(3)		0.939		
	AVG.(PY-PO)	(2)		0.939	417°	-6.82
80-70K	A*	12	Py,Cpy,Marc	0.954	<300°	-
	C	10	Py,Cpy,Marc	0.945	341°	-9.53

* - Excluded from the average as the sulfur peak drifted during the analyses.

APPENDIX II - MICROPROBE ANALYSES - PYRRHOTITE (cont.)

SAMPLE	"SPOT"	# OF ANAL.	COEXISTING SULFIDES	N_{FeS}	T(°C)	LOG $f(S_2)$
			NEW BERLIN HIGH SCHOOL (cont.)			
80-70N	A	11	2Py	0.938		
	AA	5	Py,Cpy,2Py	0.939	417°	-6.82
	B	10	Marc,Cpy	0.937		
	AVG.	(3)		0.938		
80-70PP	A	4	Py,Cpy,Marc	0.957	<300°	-
	B	11	Cpy	0.952		
	C	14	Py,Cpy	0.951	<300°	-
	D	6	Py,Cpy	0.959	<300°	-
	AVG.	(4)		0.955		
	AVG.(PY-PO)	(3)		0.956	<300°	-
80-70T	A	6	Py,Cpy,Marc	0.936	450°	-5.78
	B	11	Marc	0.938		
	C	21	Py,Cpy,marc	0.944	354°	-9.00
	AVG.	(3)		0.939		
	AVG.(PY-PO)	(2)		0.940	404°	-7.22

APPENDIX II - MICROPROBE ANALYSES - PYRITE

SAMPLE	"SPOT"	# OF ANAL.	COEXISTING SULFIDES	MOLE % Fe*	MOLE % Co*	TOTAL Co+Fe
			BLOODS BROOK			
77-23D	A	4	Po,Marc	0.985	0.017	1.002
	B	3	Po,Marc	1.002	N. A.	1.002+
	AVG.	(2)		0.994	0.017	1.011
			MT. FINISH QUARRY			
77-15Y	B	1	Po	1.046	0	1.046
	C	3	Po	1.006	0.003	1.009
	E	6	Po,Cpy	1.106	0.002	1.108
	AVG.	(3)		1.023	0.002	1.025
			CLOUGH BROOK			
77-18M	A	6	Po,Cpy	0.991	0.035	1.026
	B	6	-	1.024	-	1.024
	BB	3	-	1.015	0.001	1.016
	AVG.	(2)		1.005	0.018	1.023
77-18O	ABSENT					
77-18P	ABSENT					
77-18X1	A	6	Po,Cpy	1.011	0.003	1.014
	B	PBNA				
			WILDER DAM			
77-20G	ABSENT					
77-20N	ABSENT					
			MT. CUBE QUADRANGLE			
73-22E	B	4	Po,Cpy	0.963	0.022	0.985

* - Mole % Fe and Co are based on two moles sulfur.

APPENDIX II - MICROPROBE ANALYSES - PYRITE (cont.)

SAMPLE	"SPOT"	# OF ANAL.	COEXISTING SULFIDES	MOLE % Fe*	MOLE % Co*	TOTAL Co+Fe
			MT. CUBE QUADRANGLE (cont.)			
73-25A	A	3	Po	0.974	NA	0.974+
	B	4	Po	1.002	NA	1.002+
	AVG.	(2)		0.988	NA	0.988+
73-25B	A	2	Po,Cpy	0.957	0.031	0.988
	G	4	Cpy	1.006	0.002	1.008
	AVG.	(2)		0.982	0.017	0.999
73-26A	ABSENT					
73-27C	B	2	Cpy	0.998	0.003	1.001
	C	2	Po,Cpy	0.998	0.003	1.001
	D	2	-	1.005	0.003	1.008
	AVG.	(3)		1.000	0.003	1.003
73-30M	ABSENT					
73-31B	A	5	Po,Cpy	0.980	0.019	0.999
	B	3	Po,Cpy	0.986	0.024	1.010
	AVG.	(2)		0.983	0.022	1.005
77-58D	A	7	Po,Cpy	0.938	0.051	0.989
	B	5	Po,Cpy,Marc	0.978	0.023	1.001
	C	5	Po,Cpy	0.972	0.021	0.993
	E	4	Po,Cpy	0.970	0.030	1.000
	AVG.	(4)		0.975	0.024	0.999
			NORTH GRANTHAM			
80-28O	ABSENT					
80-28T	ABSENT					
80-28U	ABSENT					

* - Mole % Fe and Co are based on two mole sulfur

APPENDIX II - MICROPROBE ANALYSES - PYRITE (cont.)

SAMPLE	"SPOT"	# OF ANAL.	COEXISTING SULFIDES	MOLE % Fe*	MOLE % Co*	TOTAL Co+Fe
			NORTH GRANTHAM (cont.)			
80-28W	A	7	Po,Cpy	0.985	0.002	0.987
	CC	5	-	0.990	0.002	0.992
	AVG.	(2)		0.988	0.002	0.990
80-28X	B	4	-	0.974	0.007	0.982
			NEW BERLIN HIGH SCHOOL			
80-70C	A	3	Marc,2Py	1.010	0.002	1.012
	B	4	Po,Cpy	1.009	0.004	1.013
	AVG.	(2)		1.010	0.003	1.013
80-70J	A	10	Po,Cpy	1.003	NA	1.003+
	B	7	Po,Cpy	1.014	NA	1.014+
	AVG.	(2)		1.009	NA	1.009+
80-70K	A	PBNA				
	C	PBNA				
80-70N	AA	6	Po,Cpy,2Py	0.988	~0.05	1.038
80-70PP	A	3	Po,Cpy,Marc	0.999	<0.005	0.999
	C	3	Po,Cpy	0.991	~0.02	1.011
	D	3	Po,Cpy	1.026	~0.05	1.076
	AVG.	(3)		1.005	~0.025	1.030
80-70T	A	4	Po,Cpy,Marc	1.005	<0.005	1.005
	C	4	Po,Cpy,Marc	1.015	NA	1.015+
	AVG.	(2)		1.101	0.000+	1.101+

* - Mole % Fe and Co are based on two moles sulfur.

APPENDIX II - MICROPROBE ANALYSES - MARCASITE

SAMPLE	"SPOT"	# OF ANAL.	COEXISTING SULFIDES	MOLE % Fe*	MOLE % Co*	TOTAL Co+Fe
			BLOODS BROOK			
77-23D	PBNA					
			MT. FINISH QUARRY			
77-15Y	ABSENT					
			CLOUGH BROOK			
77-18M	PBNA					
77-18O	ABSENT					
77-18P	ABSENT					
77-18X1	ABSENT					
			WILDER DAM			
77-20G	ABSENT					
77-20N	ABSENT					
			MT. CUBE QUADRANGLE			
73-22E	PBNA					
73-25A	C	4	Cpy	0.996	NA	0.996+
73-25B	ABSENT					
73-26A	PBNA					
73-27C	ABSENT					

* - Mole % Fe and Co are based on two moles sulfur.

APPENDIX II - MICROPROBE ANALYSES - MARCASITE (cont.)

SAMPLE	"SPOT"	# OF ANAL.	COEXISTING SULFIDES	MOLE % Fe*	MOLE % Co*	TOTAL Co+Fe
			MT. CUBE QUADRANGLE (cont.)			
73-30M	PBNA					
73-31B	ABSENT					
77-58D	PBNA					
			NORTH GRANTHAM			
80-28O	ABSENT					
80-28T	ABSENT					
80-28U	ABSENT					
80-28W	AA**	2	Po	0.967	0.002	0.969
	B	6	-	0.995	0.002	0.997
	C**	2	Po	0.949	0.002	0.951
	AVG.	(3)		0.970	0.002	0.972
80-28X	A	6	Po	1.030	0.002	1.032
	C	4	Po	1.019	0.003	1.023
	AVG.	(2)		1.025	0.003	1.028
			NEW BERLIN HIGH SCHOOL			
80-70C	A***	4	Py,2Py	1.019	0.002	1.021
	C	1	Po	1.033	0.002	1.034
	AVG.	(2)		1.026	0.002	1.028
80-70J	ABSENT					

* - Mole % Fe and Co are based on two moles sulfur.

** - A poor surface polish resulted in low totals for the microprobe analyses.

*** - "Intermediate product" analyses.

APPENDIX II - MICROPROBE ANALYSES - MARCASITE (cont.)

SAMPLE	"SPOT"	# OF ANAL.	COEXISTING SULFIDES	MOLE % Fe*	MOLE % Co*	TOTAL Co+Fe
			NEW BERLIN HIGH SCHOOL (cont.)			
80-70K	PBNA					
80-70N	B	5	Po,Cpy	1.021	NA	1.021+
80-70PP	A	3	Po,Py,Cpy	1.009	<0.005	1.009
80-70T	A	4	Po,Py,Cpy	1.026	<0.005	1.026
	B	3	Po	1.015	<0.005	1.015
	C	3	Po,Py,Cpy	1.031	NA	1.031+
	AVG.	(3)		1.024	0.000	1.024

* - Mole % Fe and Co are based on two moles sulfur.

APPENDIX II - MICROPROBE ANALYSES - SECONDARY "PYRITE"

SAMPLE	"SPOT"	# OF ANAL.	COEXISTING SULFIDES	MOLE % Fe*	MOLE % Cu*	TOTAL Cu+Fe
			NEW BERLIN HIGH SCHOOL			
80-70C	A	9	Py,Marc**	1.015	0.002	1.017
80-70N	A	9	Po	1.012	NA	1.012+
	AA	11	Po,Py,Cpy	1.015	<0.005	1.015

* - Mole % Fe and Cu are based on two moles sulfur.

** - "Intermediate product", see text for explanation.

APPENDIX II - MICROPROBE ANALYSES - CHALCOPYRITE

SAMPLE	"SPOT"	# OF ANAL.	COEXISTING SULFIDES	MOLE % Fe*	MOLE % Cu*	TOTAL Cu+Fe
			BLOODS BROOK			
77-23D	C	2	Po,Marc	1.027	1.008	2.036
			MT. FINISH QUARRY			
77-15Y	D	1	Po	1.008	0.988	1.996
	E	2	Po,Py	1.021	1.007	2.028
	AVG.	(2)		1.015	0.998	1.007
			CLOUGH BROOK			
77-18M	A	2	Po,Py	1.049	1.032	2.081
77-18O	A	3	Po	1.018	0.991	2.008
	B	2	Po	1.014	0.999	2.013
	C	2	Po	1.031	0.976	2.007
	AVG.	(3)		1.021	0.989	2.009
77-18P	PBNA					
77-18X1	A	PBNA				
	B	2	Po,Pent,Py	1.025	1.029	2.057
			WILDER DAM			
77-20G	PBNA					
77-20N	E	1	PO	1.076	1.000	2.076
			MT. CUBE QUADRANGLE			
73-22E	A	PBNA				
	B	5	Po,Py	1.011	1.015	2.026
	D	3	Po,Marc	1.007	0.995	2.002
	AVG.	(2)		1.009	1.005	2.014

* - Mole % Fe and Cu are based on two moles sulfur.

APPENDIX II - MICROPROBE ANALYSES - CHALCOPYRITE (cont.)

SAMPLE	"SPOT"	# OF ANAL.	COEXISTING SULFIDES	MOLE % Fe*	MOLE % Cu*	TOTAL Cu+Fe
			MT. CUBE QUADRANGLE (cont.)			
73-25A	C	3	Marc	1.002	1.013	2.015
73-25B	A	2	Po,Py	1.041	0.976	2.017
	G	4	Py	1.059	0.958	2.017
	AVG.	(2)		1.050	0.967	2.017
73-26A	F	2	Po	1.031	0.999	2.030
	I	1	Po	1.010	1.002	2.012
	AVG.	(2)		1.021	1.001	2.022
73-27C	B	1	Py	1.012	0.969	1.981
	C	1	Po,Py	1.025	0.947	1.972
	AVG.	(2)		1.019	0.958	1.977
73-30M	PBNA					
73-31B	A	2	Po,Py	1.039	1.008	2.047
	B	2	Po,Py	1.039	0.989	2.028
	AVG.	(2)		1.039	0.999	2.038
77-58D	A	2	Po,Py	1.012	0.970	1.982
	B**	2	Po,Py,Marc	0.999	0.973	1.972
	C	1	Po,Py	1.011	0.967	1.978
	AVG.	(3)		1.007	0.970	1.977
			NORTH GRANTHAM			
80-28O	AA	2	Po	1.015	0.997	2.012
80-28T	AAA	2	Po	1.025	0.913	1.938
80-28U	A	2	Po	1.012	0.990	2.002
	B	3	Po	1.025	0.996	2.020
	C	2	Po	1.010	0.973	1.983
	AVG.	(3)		1.016	0.986	2.002

* - Mole % Fe and Cu are based on two moles sulfur.

** - Low totals resulted from small grain size.

APPENDIX II - MICROPROBE ANALYSES - CHALCOPYRITE (cont.)

SAMPLE	"SPOT"	# OF ANAL.	COEXISTING SULFIDES	MOLE % Fe*	MOLE % Cu*	TOTAL Cu+Fe
			NORTH GRANTHAM (cont.)			
80-28W	A	1	Po,Py	1.019	0.948	1.967
80-28W	PBNA					
			NEW BERLIN HIGH SCHOOL			
80-70C	B	2	Po,Py	1.030	0.999	2.029
80-70J	A	7	Po,Py	1.027	1.002	2.029
	B	2	Po,Py	1.040	1.012	2.052
	AVG.	(2)		1.034	1.007	2.041
80-70K	A	3	Po,Py	1.054	1.034	2.088
80-70N	AA	4	Po,Py,2Py	1.020	1.005	2.024
	B	3	Po,Marc	1.029	0.999	2.027
	AVG.	(2)		1.025	1.002	2.026
80-70PP	A	3	Po,Py,Marc	1.036	1.023	2.059
	B	3	Po	1.041	1.025	2.066
	C	3	Po,Py	1.035	1.022	2.057
	D	2	Po,Py	1.038	1.025	2.063
	AVG.	(4)		1.038	1.024	2.062
80-70T	A	3	Po,Py,Marc	1.010	1.016	2.026
	C	3	Po,Py,Marc	1.028	1.015	2.043
	AVG.	(2)		1.019	1.015	2.034

* - Mole % Fe and Cu are based on two moles sulfur.

APPENDIX II - MICROPROBE ANALYSES - PENTLANDITE

Formula - $(Fe_{3.41}Ni_{5.58}Cu_{0.13})S_8$

based on the average of 3 analyses of a single grain in 77-18X1, "spot" B

Pyrite, pyrrhotite, and chalcopyrite are present in "spot" B, but are not touching pentlandite.

APPENDIX III - SULFIDE MODAL ABUNDANCES

Key: Py → Pyrite

Po → Pyrrhotite

Cpy → Chalcopyrite

\- → absent

\+ → rare : X < 0.2%

++ → common : 0.2% ≤ X < 2.0%

+++ → abundant : 2.0% < X

INTERSTATE 91

SAMPLE #	Py	Po	Cpy
80-J5	-	++	+
J9	+++	-	+
J10	++	-	+
K1	+	-	-
K2	+	-	++
K4	++	-	+
K5	-	++	+
TOTALS	9	4	7

PY / PY + PO = 0.692

APPENDIX III - SULFIDE MODAL ABUNDANCES (cont.)

BLOODS BROOK

SAMPLE #	Py	Po	Cpy
77-22A	++	-	+
22D	+	-	+
23B	-	-	-
23D	++	++	+
24A	+	-	+
24E	-	-	-
27A	-	-	-
27B	-	-	-
28D	-	-	-
28I	-	-	-
29B	++	-	++
29H	++	-	+
30F	++	-	+
31A	+	-	-
31B	+	-	-
32B	-	-	-
TOTALS	14	2	8

PY / PY + PO = 0.875

APPENDIX III - SULFIDE MODAL ABUNDANCES (cont.)

MT. FINISH QUARRY

SAMPLE #	Py	Po	Cpy
77-15A	-	-	-
15B	-	-	-
15D	+	-	+
15E	+	-	+
15F	+	-	+
15I	-	-	+
15L	-	-	-
15M	+++	-	++
15O	++	-	+
15P	++	-	+
15Q	+	-	+
15W	+	-	+
15X	+	-	+
15X1	+	-	+
15Y	+	++	+
15Z	-	-	-
76-7O	+	-	-
TOTALS	16	2	13

PY / PY + PO = 0.889

APPENDIX III - SULFIDE MODAL ABUNDANCES (cont.)

CLOUGH BROOK

SAMPLE #	Py	Po	Cpy
77-18A	+	-	+
18C	-	-	-
18D	-	-	-
18E	-	-	-
18G	-	-	-
18H	-	-	-
18I	-	-	-
18J	-	-	-
18K	+	-	-
18L	-	-	-
18M	+	+	+
18N	-	+	-
18O	-	+	+
18P	-	+++	+
18Q	-	-	-
18R	-	-	-
18T	-	+	-
18U2	-	-	-
18U3	-	-	-
18V1	-	-	-
18X1	++	+	+
TOTALS	5	8	5

PY / PY + PO = 0.385

APPENDIX III - SULFIDE MODAL ABUNDANCES (cont.)

WILDER DAM

SAMPLE #	Py	Po	Cpy
77-20C	-	++	+
20D	-	++	+
20E	-	++	+
20F	+	++	+
20G	-	++	+
20H	-	++	+
20I	-	++	+
20J	+	+	+
20K	-	++	+
20M	-	+	+
20N	-	+	+
20O	-	++	+
TOTALS	2	21	12

PY / PY + PO = 0.087

APPENDIX III - SULFIDE MODAL ABUNDANCES (cont.)

MT. CUBE QUADRANGLE

SAMPLE #	Py	Po	Cpy
73-20A	+	-	+
21B	-	-	-
22E	+	++	+
23C	-	-	-
24A	++	-	+
25A	++	++	+
25B	++	+	+
26A	-	+	+
27C	+	+	+
28B	-	-	-
29D	++	-	+
30A	-	++	-
30C	-	-	-
30J	-	+++	+
30M	-	++	+
30O	-	+	+
30R	+	-	+
31A	-	-	-
31B	+	++	+
31G	-	-	-

APPENDIX III - SULFIDE MODAL ABUNDANCES (cont.)

MT. CUBE QUADRANGLE (cont.)

SAMPLE #	Py	Po	Cpy
73-31K	-	-	-
79-56A	-	-	-
56B	-	-	-
56C	-	-	-
57	+	-	-
58D	++	++	+
TOTALS	16	19	14

PY / PY + PO = 0.457

APPENDIX III - SULFIDE MODAL ABUNDANCES (cont.)

NORTH GRANTHAM

SAMPLE #	Py	Po	Cpy
80-28A	-	-	-
28B	-	-	-
28C	-	-	-
28D	-	-	-
28E	-	-	-
28F	-	-	-
28G	+	-	+
28H	-	-	-
28I	-	-	-
28J	-	-	-
28K	-	+	+
28L	+	++	+
28M	-	-	-
28N	-	++	+
28O	-	++	+
28P	-	-	-
28Q	-	-	-
28R	-	-	-
28S	-	-	-
28T	-	++	+

APPENDIX III - SULFIDE MODAL ABUNDANCES (cont.)

NORTH GRANTHAM (cont.)

SAMPLE #	Py	Po	Cpy
80-28U	-	+++	+
28V	+	+	+
28V1	-	+	-
28W	+	++	+
28X	+	+	+
28Y	-	++	+
28Z	+	-	-
28AA	-	-	-
28BB	+	-	-
28CC	-	-	-
TOTALS	7	19	11

PY / PY + PO = 0.269

APPENDIX III - SULFIDE MODAL ABUNDANCES (cont.)

NEW BERLIN HIGH SCHOOL

SAMPLE #	Py	Po	Cpy
80-70A	+	-	+
70B	++	-	+
70C	++	+++	+
70D	-	-	-
70E	-	-	-
70F	+	+	-
70G	+	+	+
70H	-	-	-
70I	+	++	+
70J	+++	++	+
70K	+++	+++	+++
70L	++	+	+
70M	++	++	+
70N	++	++	+
70O	+	-	-
70P	+	++	-
70PP	++	+++	++

APPENDIX III - SULFIDE MODAL ABUNDANCES (cont.)

NEW BERLIN HIGH SCHOOL (cont.)

SAMPLE #	Py	Po	Cpy
80-70Q	++	++	+
70R	++	+++	+
70S	+	++	+
70T	++	+++	++
70U	+	++	+
70V	-	-	-
TOTALS	32	34	20

PY / PY + PO = 0.485

APPENDIX IV - POINTS ON PYRITE-PYRRHOTITE EQUILIBRIUM CURVE (ILLUSTRATED IN FIGURE 16)

N_{FeS}	T(°C)	Log $f(S_2)$
0.920	602	-1.95
0.921	592	-2.16
0.922	583	-2.36
0.923	574	-2.56
0.924	566	-2.76
0.925	557	-2.96
0.926	548	-3.17
0.927	539	-3.39
0.928	530	-3.61
0.929	521	-3.83
0.930	512	-4.05
0.931	502	-4.32
0.932	492	-4.59
0.933	482	-4.86
0.934	472	-5.16
0.935	461	-5.47
0.936	450	-5.78
0.937	439	-6.11
0.938	428	-6.46
0.939	417	-6.82
0.940	404	-7.22
0.941	391	-7.68
0.942	378	-8.13
0.943	366	-8.57
0.944	354	-9.00
0.945	341	-9.53

taken from Toulmin and Barton (1964)

APPENDIX V - MICROPROBE ANALYSES - SILICATES AND OXIDES

SILICATE	SAMPLE	-1- FE/FE+MG	-2- FE/FE+MG
Biotite	80-28O	0.362	0.360
	80-28W	0.451	0.436
Hornblende	80-28O	0.384	0.367
Cummingtonite	77-18O	0.498	0.499

FE/FE+MG ratio is calculated in mole percent.

Ratios in column -1- represent the averages of several analyses taken as close to a pyrrhotite grain as possible.

Ratios in column -2- represent the average of several analyses in the same grain taken at a distance from the pyrrhotite grain.

- -

ILMENITE	SAMPLE	-1- FE/FE+TI	-2- FE/FE+TI
	77-23D	0.507	0.501
	77-18O	0.504	0.522
	77-20N	0.491	0.498
	73-25A	0.529	0.538
	73-26A	0.517	0.521
	73-31B	0.491	0.492
	80-28W	0.522	0.531

FE/FE+TI ratio is calculated in mole percent.

Ratios in column -1- represent average analyses for ilmenite grains close to, or touching, pyrrhotite grains.

Ratios in column -2- represent average analyses for ilmenite grains in pyrrhotite-free areas.